REPORT –

Development of a Hydrogeologic Framework for Karnes and Wilson Counties Based on the Analysis of Geophysical Logs

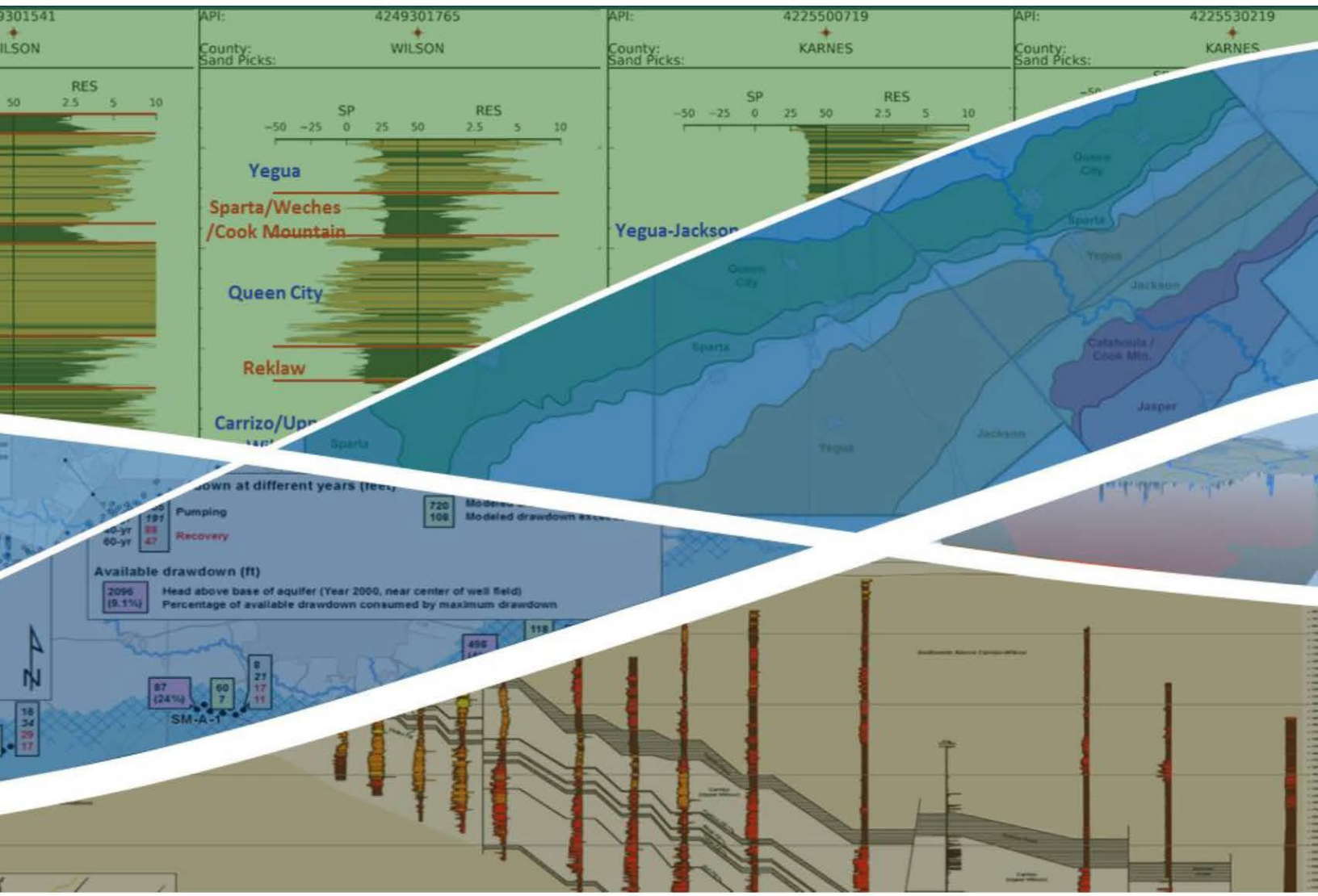

Prepared For

EUWCD

Prepared By

INTERA
GEOSCIENCE & ENGINEERING SOLUTIONS

January 2017

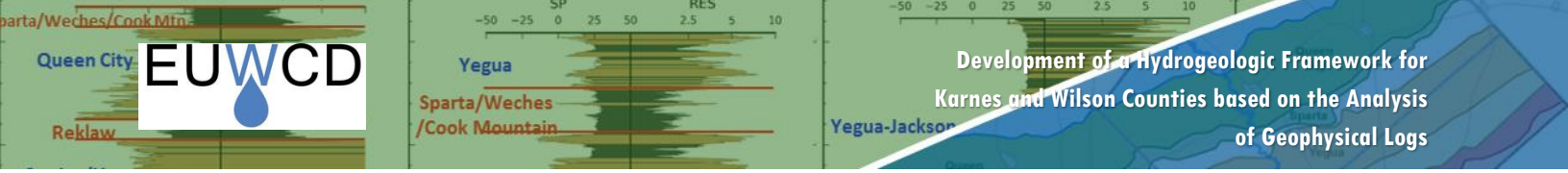

DEVELOPMENT OF HYDROGEOLOGIC FRAMEWORK FOR KARNES AND WILSON COUNTIES BASED ON THE ANALYSIS OF GEOPHYSICAL LOGS

Prepared for:

Evergreen Underground Water Conservation District
11 Wyoming Boulevard
Pleasanton, TX 78064
830.569.4186

Prepared by:

Daniel Lupton, PG
Steven Young, PE, PG, PhD

And

Scott Hamlin, PG, PhD

January 2017

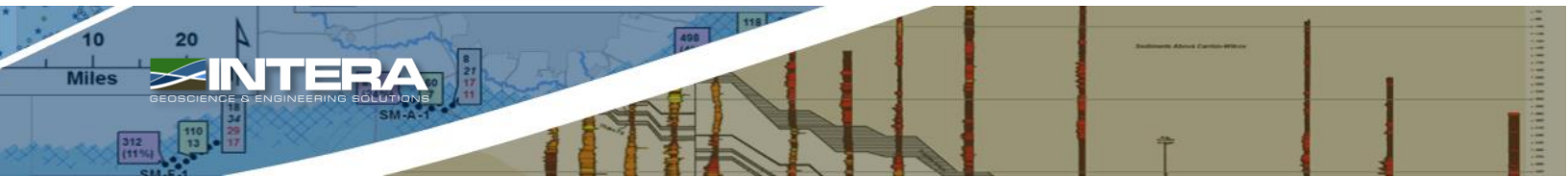

EXECUTIVE SUMMARY

The study analyzed 95 geophysical logs to create five cross-sections through Karnes and Wilson counties. The cross-sections include three dip cross-sections and two strike cross-sections. The cross-sections show the stratigraphic boundaries, shale layers, and different water quality classifications of groundwater in the sand layers for the Carrizo-Wilcox Aquifer, the Queen City Aquifer, the Sparta Aquifer, the Yegua-Jackson Aquifer, and the Gulf Coast Aquifer System. The stratigraphic boundaries for the Carrizo-Wilcox Aquifer are based on a chronostratigraphic framework. This framework was used to map ten major transgressive shales that are key markers and boundaries for delineating the Carrizo-Wilcox Aquifer. Three of these shales are located in the Middle Wilcox and they jointly act as an effective barrier to groundwater flow between the Carrizo/Upper Wilcox Aquifer and the Lower Wilcox Aquifer. One of the shales that was mapped but is above the Carrizo-Wilcox Aquifer is the Reklaw formation. The Reklaw formation is typically more than 200 feet thick, is easily traceable between logs, and serves as an effective hydrogeologic barrier to groundwater flow between the Queen City Aquifer above it and the Carrizo/Upper Wilcox Aquifer below it. In addition, the shales associated with the Cook Mountain were mapped and these shales serve to isolate the Yegua-Jackson from aquifers below it.

For all 95 geophysical logs, the resistivity/induction and the spontaneous potential curves were analyzed to identify continuous sequences of sands and clays above the base of the Carrizo-Wilcox Aquifer to the top of the log. A total of 3,527 sand intervals were identified. For each of the sand interval, the total dissolved solids (TDS) concentration of the groundwater in the sand was estimated based on the resistivity value of the sand interval. The TDS concentrations calculated from the resistivity values were used to group the water quality of the groundwater into the following classifications: fresh water (TDS concentration less than 1,000 mg/L), slightly saline (TDS concentration between 1,000 and 3,000 mg/L), moderately saline (TDS concentration between 3,000 and 10,000 mg/L), and very saline (TDS concentration above 10,000 mg/L).

Faults were also mapped in the three dip cross-sections. Despite offsets across the faults of up to 700 feet, groundwater appears to flow through the faults while primarily remaining in the same formation. The continuity of the groundwater flow through a fault within a single formation is indicated by gradual and small changes in the water quality within the different formations across a fault. The continuity in TDS concentrations across faults is most evident in the Carrizo/Upper Wilcox Aquifer, which is a smaller aquifer within the Carrizo-Wilcox Aquifer. The Carrizo/Upper Wilcox Aquifer also contains freshwater at much greater depths than any formation. In the furthest southwest dip cross-section of the Carrizo/Upper Wilcox Aquifer, freshwater occurs to depths approaching 4,000 feet in the Carrizo-Wilcox Aquifer and slightly saline groundwater occurs at depths near 6,000 feet.

GEOSCIENTIST AND/OR PROFESSIONAL ENGINEER SEAL(S)

Daniel Lupton, P.G.

Daniel Lupton was responsible picking the sand and clay intervals for the geophysical logs, and responsible for developing and implementing a methodology for calculating total dissolved solids concentrations based on the resistivity of the formation and writing portions of the report.

01/24/2017

Steven C. Young, P.E., P.G., Ph.D.

Dr. Steven Young was the project manager and was primarily responsible for writing the report, checking the log analysis for consistency and accuracy, and developing an approach for integrating data from several projects.

01/24/2017

Scott Hamlin, P.G., Ph.D.

Dr. Hamlin was responsible for selecting the logs for the cross-sections, for correlating the transgressive shales in Karnes County, and for delineating the stratigraphic boundaries that delineate the Wilcox Aquifer.

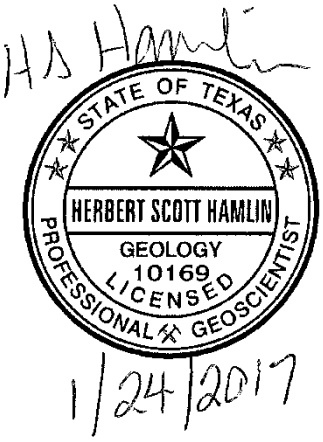

01/24/2017

TABLE OF CONTENTS

LIST OF FIGURES

LIST OF TABLES

ACROYNMS AND ABBREVIATIONS

API	American Petroleum Institute
cm	centimeters
Cz	Carrizo lithology
Czo	Carrizo Formation
Du	Dull Shale
EUWCD	Evergreen Underground Water Conservation District
GAM	Groundwater Availability Model
GMA	Groundwater Management Area
Hb	Hobson Shale
INTERA	INTERA Incorporated
Kn	Kenedy Shale
LMF	Lower Mixed Facies of Carrizo Formation
L. Wx	Lower Wilcox Subgroup
M. Wx	Middle Wilcox Subgroup
mg/L	milligrams per liter
ohm-m	ohm-meters per meter
ohm^2/m	square ohm-meters per meter
Psh	Poth Shale
QC	Queen City Formation and/or lithology
R1	Reklaw 1
Rn	Runge
STEER	South Texas Energy and Economic Roundtable
SP	Spontaneous potential
Td	Tilden Shale
TDS	total dissolved solids
TWDB	Texas Water Development Board
UMF	Upper Mixed Facies of Carrizo Formation
Wb	Webb Shale
We	Weches Formation
Yk	Yoakum Shale

1.0 INTRODUCTION

The Evergreen Underground Water Conservation District (EUWCD) includes Atascosa, Frio, Karnes, and Wilson counties. The District manages its groundwater resources with the goal of conserving the resources while seeking to maintain the economic viability of all water resource user groups, public and private. In consideration of the economic and cultural activities occurring within the District, the District identifies and promotes best management practices of all groundwater resources within the District. In pursuit of its mission to promote best management practices, the District supports technical studies to improve the characterization and modeling of its groundwater resources.

1.1 Background Information

In August 2016, the EUWCD funded INTERA Incorporated (INTERA) to conduct this study. An objective of the study is to provide hydrogeological information helpful for improving the management of groundwater resources in the District. The study's primary task was to integrate and expand on recent projects involving analysis of well logs located in Karnes and Wilson counties, with the goal of constructing a hydrogeological framework for Karnes and Wilson counties that would help the development of prudent groundwater management policies. The components of the hydrogeological framework include stratigraphic picks that delineate the major and minor aquifers, lithologic picks that identify the location of major intervals of sands or clays, and water quality picks that map the major salinity zones in the minor and major aquifers. Three of the recent projects from which this study relied on for hydrogeological data and geophysical log analysis are: (1) an EUWCD-funded project focused on developing a detailed stratigraphy of the Carrizo-Wilcox Aquifer underlying Wilson and Atascosa counties; (2) a Texas Water Development Board (TWDB)-funded project focused on delineating the stratigraphy and characterizing groundwater quality of the Carrizo-Wilcox Aquifer in GMA 13; and, (3) a South Texas Energy and Economic Roundtable (STEER)-funded project focused on assembling and integrating hydrogeological data to support the improving aquifer characterization of the major and minor aquifers in EUWCD.

The study involves the analysis of 95 geophysical logs to delineate stratigraphy, sand and clay intervals, and the total dissolved solids (TDS) concentrations in groundwater along five vertical cross-sections in Wilson and Karnes counties. **Figure 1** shows the location of the five cross-sections. Three of the cross-sections are aligned along geologic dip and two of the cross-sections are aligned along geologic strike.

1.2 Report Organization

The report includes two main sections and a summary. **Section 2** provides an introduction and background information describing geophysical logs. The primary log types used as part of this study are resistivity/induction and spontaneous potential. **Section 3** describes the methodology used for the log analysis and presents plots of stratigraphy, lithology, and water quality along five cross-sections. The information present in the plots are consistent with results from several previous studies, including Hargis (2015a,b; 2009) and Hamlin and others (2016). **Section 4** provides a brief summary of the findings, while **Section 5** includes a list of references.

2.0 GEOPHYSICAL LOGS

Borehole geophysics involves recording and analyzing physical and electrical property measurements made in a borehole (or a well). Geophysical measurements are made by lowering a sonde into the borehole on the end of an electric cable. The majority of the work associated with this study involves the assembling and analysis of geophysical logs to evaluate physical and electronic signatures in support of the characterization of aquifer stratigraphy, lithology, and water quality.

2.1 Types of Borehole Geophysical Logs

Because the first geophysical borehole logs were made more than seventy years ago, a number of probes have been developed to measure nearly every possible physical parameter in a borehole. The different logging tools are not named according to any particular system. Some are named on the basis of the parameter measured, others according to the principle by which the measurement is made, and still others on the basis of the geometry of the probe or the trade name. **Table 2-1** summarizes basic information on the most important and widely applied logging tools in hydrogeology.

Table 2-1 General description of types of geophysical logs

Log type	Specific log	Borehole Conditions	Information
Nuclear	Gamma-ray Gamma-gamma (density) Neutron-neutron (porosity)	Open and cased holes with or without fluid Open holes with fluid	Lithology, density, porosity, calibration of surface geophysics
Electrical	Spontaneous Potential Resistivity Focused Resistivity	Open or screened holes with fluid	Lithology, salinity of groundwater, calibration of surface geophysics, location of PVC screens
Electromagnetic	Induction Nuclear magnetic resonance	Open and PVC cased holes with or without fluid	Lithology, salinity of groundwater
Acoustical	Sonic	Open holes with fluids	Lithology (porosity)
Optical	Borehole camera Optical borehole televiewer	Borehole camera Optical borehole televiewer	Borehole camera Optical borehole televiewer
Flow	Impeller flowmeter Heat pulse flowmeter	Open and cased holes with fluid	Vertical water movement in the borehole
Fluid	Water quality	Open and cased holes with fluid	EC, temperature, pH, O_2, NO_3, Eh, total gas pressure

The three types of geophysical logs used that were analyzed as part of this the study are resistivity, induction, and spontaneous potential (SP). Each of these types of geophysical logs are described in the following subsections.

2.1.1 Resistivity Log

In conventional resistivity logging, an electric current is forced to flow between two electrodes, and the resulting electric potential (voltage) is measured between two other electrodes. Resistivities of surrounding geologic material is computed from the voltage measurement. The unit of resistivity (reciprocal of conductivity) measurement is the square ohm-meter per meter (ohm^2/m).

Dry formations will have very high resistivities because they are poor conductors of electricity. Saturation of a deposit reduces its resistivity because water is an electrical conductor. In general, saturated subsurface materials with low resistivity include silts, clays, and shales. Fresh water deposits composed of sands and gravel tend to have high resistivities. The resistivity of a formation will vary inversely with the TDS concentrations in its pore water. One of the reasons that clays tend to have low apparent resistivities is because their interstitial waters are often highly mineralized. On the other hand, sands and gravels saturated with fresh water tend to have high apparent resistivities because their surfaces are relatively inert and tend to release few minerals into solution.

Figure 2 illustrates how apparent resistivity can vary with differences in subsurface material and TDS concentration in groundwater. The difference in apparent resistivity between sandy and clayey deposits is considerably greater in fresh water than in very brackish water. In fact, in salt water, the difference in apparent resistivity between clay and sand is subtle. In situations that involve heterogeneous deposit types and vertical variations in water quality, analysis of the resistivity logs should be performed in concert with the analysis of other logs that provide independent information on either the characteristics of the deposits or the water quality.

Because the borehole fluids affect the resistivity measurement, the borehole diameters should be kept as small as possible. In a large-diameter hole or with short spacings between the electrodes, the resistivity will be heavily influenced by the drilling fluid. This is because the "zone of influence" of the electrodes may not extend very far into the formation (Driscoll, 1986). To help identify and account for the influence of the borehole fluids, several electrodes spacings may be used to obtain different degrees of penetration into the surrounding geological material. The resistivity logs that were most commonly analyzed for this study consist of two electrodes downhole. When the separation of the electrodes is 16 inches or less, the configuration is called a short normal. If the two electrodes are separated by 64 inches, the configuration is called a long normal. The larger the spacing between the two downhole electrodes, the deeper the penetration of the measurement into the formation.

2.1.2 Induction Logs

Induction logs provide similar information as do resistivity logs. However, the induction logging tool can be used in dry boreholes, in boreholes containing nonconducting fluids, and in polyvinyl chloride-cased boreholes, whereas resistivity tools cannot.

Instead of using electrodes to generate electric current in the subsurface, a borehole induction tool uses electric coils to create magnetic fields that in turn induce electric currents in the subsurface. The induced electrical eddy currents are proportional to the conductivity of the rock. An induction tool usually contains two coil systems with different coil spacings and thus different investigation depths. Coil systems with several transmitter and receiver coils are used to focus the field to minimize the influence of the borehole itself on the recorded signal. The investigation depth depends on the conductivity of the rock and is 60 – 350 centimeters (cm) for a dual induction log.

2.1.3 Spontaneous Potential Log

Spontaneous potential (SP) logs record naturally occurring electrical potentials (voltages) that occur in the borehole at different depths. The SP log primarily measures the electrochemical potential between a stationary reference at the surface and a moving electrode in the borehole.

The circuitry between the surface and the downhole electrode does not include an external source for an electric current. The electrochemical potential is generated by ions moving between the borehole fluid and the formation water. If there is no contrast in the ionic concentrations of the borehole fluid and the formation water, there is no electrochemical potential, and therefore the SP potential is zero. The downhole electrode usually has a lower (more negative) potential than the surface electrode. SP logs only record relative values rather than the absolute values measured by resistivity tools.

Figure 2 illustrates SP responses that can be expected in formations containing fresh water, brackish water, and salt water when the drilling fluid is composed of fresh water. As shown in Figure 2, at shallow depths where there may be little difference in the concentration of ions between the drilling fluids and the aquifer, the analysis of the SP log may be difficult because of the lack of deflections. However, at deeper depths where the formation waters are more mineralized than the drilling fluids, the leftward deflections (more negative values) in the SP logs are useful for identifying permeable strata. The analysis of an SP log begins with developing a "baseline" by connecting the potentials associated with the impermeable beds such as clays and shales as shown with the dashed line in Figure 2. Deflections to the left of this baseline are usually associated with beds of coarse-grained deposits such as sands and gravels. If no clay layers are present in the lithologic profile, the SP log may not provide much useful information.

2.2 Geophysical Logs Used for the Study

A total of 95 geophysical logs were used for this study. The logs were obtained from three sources. The primary source of logs were DVDs provided to EUWCD by Dr. Richard Hargis, who completed a multi-year study in 2015 that focused on identifying and mapping transgressive shales in the Wilcox Group. The majority of Dr. Hargis' work is summarized in two reports. Hargis (2015a) focuses on log analysis in Atascosa County, whereas Hargis (2015b) focuses on log analysis in Wilson County. The remaining logs were obtained by Dr. Scott Hamlin and INTERA from either the Bureau of Economic Geology or the Subsurface Library in Austin Texas.

Table 2-2 lists the number of logs associated with the five cross-sections. For each of the cross-sections, Table 2-2 also lists the number of logs that were also used as part of cross-sections associated with two related hydrogeologic studies of the Wilcox Aquifer. Forty-five of the logs overlap with the logs used by Hargis (2015a,b). Forty-seven of the logs were used by a TWDB-funded study to characterize the brackish groundwater associated with the Wilcox Aquifer in GMA 13. These forty-seven logs were originally obtained for the purpose of this study and were eventually incorporated by Dr. Hamlin in the analysis of logs to characterize the Wilcox Aquifer in GMA 13 (Hamlin and others, 2016). Twenty of the 95 logs for this study overlap with the logs used by Hargis (2015 a,b) and Hamlin and others (2016). All of the stratigraphic picks provided by Hargis (2015a,b) and by Hamlin and others (2016) are the same as those used in this report.

Table 2-2 Number of logs associated with each cross-section

Cross-Section	Number of Geophysical Logs			
	Total	Used by Hargis (2015a,b)	Used by Hamlin and others (2016)	Used by Hargis (2015a,b) and by Hamlin and others (2016)
Dip F-F'	22	15	11	6
Dip G-G'	25	15	14	7
Dip H-H'	22	15	10	6
Strike S1-S1'	16	0	10	0
Strike S2-S2'	15	0	5	0

3.0 CONSTRUCTION OF CROSS-SECTIONS

The cross-sections were developed using software called PETRA (IHS, 2009). PETRA is a commercial software widely used in the oil and gas industry to manage and analyze geophysical logs. All the logs were brought into PETRA as TIFF files. TIFF files are images that are created by scanning a paper copy of the geophysical logs. Prior to analyzing the TIFF files, the files were "depth registered" to facilitate the process of creating the five cross-sections. The process of depth registering involves the correcting of any distortion in the image so that accurate elevation picks can be made by marking the image.

3.1 Stratigraphy

The construction of the three dip sections began with stratigraphic picks provided by Hargis (2015a,b) for 45 logs in Wilson County. EUWCD commissioned Richard N. Hargis in November of 2008 to perform a stratigraphic analysis of the Wilcox Group for their District. Mr. Hargis' qualifications for Carrizo and Wilcox stratigraphic and structural interpretation are literally unparalleled. He has been recognized by numerous geological societies for his in-depth understanding of the Carrizo and Wilcox stratigraphic intervals. Hargis (1985, 1986) provides the general approach for the defining the stratigraphic of the Wilcox Group is south Texas. In 2009, Hargis (2009) identified the ten major transgressive shales shown in **Figure 3** as the key markers and boundaries for delineating the Wilcox Formation. The names and abbreviation of these ten shales are the Reklaw 1 (R1), Hobson (Hb), Runge (Rn), Kenedy (Kn), Clayton (Cy), Dull (Du), Yoakum (Yk), Webb (Wb), Tilden (Td) and Poth (Psh) Shales. The Hobson and Dull Shales are present only along the southeast fringe of the study area. The shales are the most extensive marine transgressions in the Wilcox in the northern portion of South Texas for a specific time horizon. These shales form the natural boundaries and likely serves as an aquitard over the area covered by the shale. **Figure 4** and **Figure 5** show the up-dip areal extent of the shales.

The 45 logs from Hargis (2015a,b) that were used as the kernel for the study are associated with the dip cross-sections F, G, and H constructed by Hargis (2015a,b) for Wilson County. The remaining logs for the study were gathered by Dr. Hamlin to extend these three cross-sections southeast of Wilson County and into Karnes County and to create two strike-oriented cross-sections in Karnes County. For the logs in Karnes County, Dr. Hamlin made the stratigraphic picks for transgressive shales based on the chronostratigraphic approach described by Hargis (2009) and for partitioning the Wilcox Aquifer into a lower, middle, and upper sections. Dr. Hamlin's stratigraphic picks for partitioning the Wilcox Aquifer were based on the work by Hargis (2009, 2015a,b) as well as by Hamlin (1988).

The stratigraphic picks made at the log locations for formations younger than the Wilcox Aquifer were made by INTERA. These stratigraphic picks include picking the top of the Yegua-Jackson Aquifer, the top of a combination of the Sparta, Weches, and Cook Mountain Formation, the top of the Queen City Formation, and the top of the Reklaw Formation. These top elevations were determined from a two-step process. The first step was to determine the elevation of the top of the formation at each log location by sampling a surface elevation map of the formation top using a geographic information system (GIS) program. The second step was to adjust the sampled elevation based on an interpretation of the log's resistivity and SP curves to the elevation that marked the top of the aquifer/formation. The GIS maps of surface elevation were obtained from databases produced from TWDB projects that develop GAMs for the aquifers and formations of interest. Surfaces for top elevations associated with the Queen City and Sparta aquifers were obtained from the Southern Central Queen City/Sparta GAM (Kelley and others, 2004). A surface for the top surface for the Yegua-Jackson Aquifer was obtained from

the GAM for the Yegua-Jackson Aquifer (Deeds and others, 2010). Surfaces for the Gulf Coast Aquifer System were obtained by surfaces developed by Young and others (2010).

Figures 6 through **10** show the five cross-sections with stratigraphy. The vertical axis is scaled to represent elevation reference to sea level. At the top of each geophysical log is the American Petroleum Institute (API) number for the log. In each of the cross-sections the shale units are colored gray as they correlate between logs. Most of these shales are continuous over their extent except in the vicinity of faults, whose locations are approximated by slanted lines across which there are offsets in the elevation of the shales. Faults in Wilson and Karnes counties were identified by Dr. Hargis and Dr. Hamlin, respectively.

3.2 Lithology

Mr. Daniel Lupton performed most of the lithology picks in PETRA. The lithology picks consisted of marking the top elevation of sands and clays sequences based on his evaluation of both the shallow resistivity, deep resistivity, and the spontaneous potential curves. A total of 3,527 sand intervals were identified on 95 logs. The digitized versions of the geophysical logs are shown in Figures 6 through 10. On the right-hand side of each log are plotted values from either a resistivity or induction log. On the left-hand side of the of each log are plotted values from the SP curve. The distance between the logs is colored to represent either sand or clay. Clay units are colored brown and sand units are color-coded based on the estimated concentration of the TDS concentration of groundwater in the sand.

3.3 Total Dissolved Solids Concentrations

For each of the sand intervals on the geophysical logs, the TDS concentrations of the groundwater were estimated based on the resistivity value for the sand intervals. The TDS concentrations calculated from the resistivity values was used to classify the water quality of the groundwater based on the classification scheme developed by Winslow and Kister (1956) and shown in **Table 3-1**. In Figures 6 through 10, the sand intervals are color-coded based on the four water classifications described in Table 3-1.

Table 3-1 Groundwater classification based on the criteria established by Winslow and Kister (1956)

Water Classification Description	TDS Range
Fresh	Less than 1,000 mg/L
Slightly Saline	1,000 to 3,000 mg/L
Moderately Saline	3,000 to 10,000 mg/L
Very Saline	10,000 to 35,000 mg/L

Note: TDS=total dissolved solids; mg/L=milligrams per liter

The TDS concentrations for the sand intervals was estimated using an approach called the Mean R_o Method, which involves calculating TDS from resistivity measurements on a geophysical log. Among the studies that have used the Mean R_o Method in either the Gulf Coast Aquifer System or the Carrizo-Wilcox Aquifer are: Fogg and Blanchard (1986), Hamlin and others (1988), Collier (1993), Estepp (1998), Hamlin and Luciana de la Rocha (2015), Ayers and Lewis (1985), Fogg (1980), Fogg and Kreitler (1982), Meyer (2012), Hamlin and others (2016), and Young and others (2016). For this study, the TDS concentrations was calculated using the Mean R_o Method using the deep resistivity (long normal or deep induction).

The development of the Mean R_o Method typically requires plotting TDS concentration measured in a water well against the resistivity (R_o) of the sands intersected by the well. Often, the geophysical log is from a borehole that was drilled near the well. **Figure 11** is a Ro-TDS graph developed by Hamlin and others (2016) for groundwater in the Carrizo/Upper Wilcox Aquifer in GMA 13. **Figure 12** is a R_o-TDS graph developed by Young and others (2016) for a groundwater in the Chicot Aquifer in the Texas Gulf Coast Aquifer System. The graph shows an inverse relationship between TDS concentration and formation resistivity. However, the relationship between TDS concentration and resistivity is substantially different for the two aquifer systems. The different relationship developed for the two aquifer systems is caused by a wide range of factors, including different sand and clay mineralogies, different depositional settings, different porosities, different groundwater chemistries, and different temperatures. These differences underscore the importance of obtaining site-specific data for developing the Mean R_o Method for an aquifer.

In both Figures 11 and 12, there is scatter of data points about the best fit line used to represent the relationship between resistivity and TDS concentration. The scatter in the data exists partly because the R_o Method does not explicitly account for differences in chemical composition of the TDS concentration, effects of mud filtrate, resolution of the logging tool, variations in the sands, and the possible inclusion of clays in the sand layer. Despite the scatter, the standard practice is to use the relationship expressed by the straight lines in Figures 11 and 12 to estimate TDS concentrations from resistivity without providing a confidence limit that would indicate a level of uncertainty with the estimate. For example, using the relationship expressed by the line in Figure 11, a resistivity of 100 ohm-meters per meter (ohm-m) and of 10 ohm-m represent TDS concentrations of 200 milligrams per liter (mg/L) and 4,000 mg/L, respectively.

For this study, the resistivity values used to assign the TDS concentrations that are used to classify groundwater based on water quality criteria are provided in **Table 3-2**. These resistivity values were obtained from three groundwater studies that included parts or all of EUWCD. Data analysis results from Hamlin and others (2016) were used to evaluate the water quality of the Carrizo and Wilcox intervals. Data analysis results from Wise (2014) were used to evaluate the water quality of the Queen City and Sparta intervals and data analysis results from Young and others (2016) were used to evaluate the water quality in the Yegua-Jackson and Gulf Coast units. Table 3-2 is a summary of the resistivity values used from these three references to create values of resistivity for calculating TDS concentration of 1,000 mg/l, 3,000 mg/L, and 10,000 mg/l for the different formations and aquifers in Figures 6 through 10.

Table 3-2 Summary of resistivity cutoff values for the various water quality categories

Aquifer	TDS (mg/L)	R_o (ohm-m)	Source
Gulf Coast	1,000	12.3	Young and others (2016) Table 13-24 (Jasper)
Gulf Coast	3,000	4.5	Young and others (2016) Table 13-24 (Jasper)
Gulf Coast	10,000	2.7	Young and others (2016) Table 13-25 (30% Porosity Calc)
Yegua-Jackson	1,000	12.3	Young and others (2016) Table 13-24 (Jasper)
Yegua-Jackson	3,000	4.5	Young and others (2016) Table 13-24 (Jasper)
Yegua-Jackson	10,000	2.7	Young and others (2016) Table 13-25 (30% Porosity Calc)
QCSP	1,000	31.1	From BRACS database for TN 14-01 (Wise, 2014)*
QCSP	3,000	11.5	From BRACS database for TN 14-01 (Wise, 2014)*
QCSP	10,000	3.9	From BRACS database for TN 14-01 (Wise, 2014)*
Carrizo	1,000	25.0	Hamlin and others (2016) Table 4-2 (NE)
Carrizo	3,000	10.0	Hamlin and others (2016) Table 4-2 (NE)
Carrizo	10,000	4.0	Hamlin and others (2016) Table 4-2 (NE)
Wilcox	1,000	33.0	Hamlin and others (2016) Table 4-3
Wilcox	3,000	16.0	Hamlin and others (2016) Table 4-4
Wilcox	10,000	11.0	Hamlin and others (2016) Table 4-5

* Data related to the relationship between formation resistivity and TDS was not available within the Wise (2014) report and was therefore acquired from the BRACS database.

Several of the R_o cutoff values in Table 3-2 are not based upon a plot of measured TDS concentration versus resistivity. In these cases, there was insufficient data to create a relationship between TDS concentrations and resistivity at the concentration value of interest, so the R_o value was calculated using the R_{wa} Minimum Method.

The development of the R_{wa} Minimum Method is beyond the scope of this study but the general formulation of the method is relevant to the study so a general overview of the method is provided. The R_{wa} Minimum method uses the Archie (1942) equation to estimate TDS concentration. For the situation where the aquifer is saturated with water, the Archie Equation can be written as:

$$R_{we} = \Phi^m \times R_o \qquad \text{(Equation 3-1)}$$

where

R_{we} = resistivity of water equivalent (ohm-meters)
Φ = porosity
m = the cementation exponent
R_o = the resistivity of a 100 percent water saturated formation (ohm-meters)
F = formation factor = Φ^m

In Equation 3-1, the cementation exponent is a function of the consolidation of the formation. Estepp (1998, 2010) provide guidelines for estimating the value of *m* for an aquifer. After Equation 3-1 has been applied to

calculate the value of $R_{we,}$ Equation 3-2 is then used to calculate a value of C_w. Equation 3-3 is then used to calculate the TDS of the groundwater based on the value C_w. Readers interested in the details associated with developing and applying the R_{wa} Minimum Method are referred to Young and others (2016), Lupton and others (2016), and Meyer and others (2014).

$$C_w = 10{,}000 / R_{we} \qquad \text{(Equation 3-2)}$$

$$TDS = ct * C_w \qquad \text{(Equation 3-3)}$$

where

C_w = specific conductance (umhos/cm at 77 degrees Fahrenheit)
ct = specific conductivity-total dissolved solids concentration conversion factor
TDS = total dissolved solids concentrations (milligrams per liter)

3.4 Discussion of Cross-Sections

The five cross-sections shown in Figures 6 through 10 are separated into three dip sections (F, G and H) and two strike sections (S1 and S2). Across most of the area covered by the logs, the Sparta Aquifer is generally sand-poor and is sandwiched between two clay rich formations, the Weches and the Cook Mountain formations. From a practical perspective, these three formations have been combined into a single layer based on high frequency of shales indicated in the geophysical logs. The single layer named Cook Mountain/Sparta/Weches represents a shaly interval that prevents vertical groundwater flow. As such, the layer is colored gray along with the ten shale units identified by Hargis (2009).

Our analysis of the five cross-sections supports a simple but useful conceptual model of the groundwater flow system. The key points associated with the schema are as follows:

- There are four primary flow systems that are separated from each other by formations that are shale rich. These primary flow systems are the Yegua-Jackson and the Gulf Coast Aquifer System, the Queen City Aquifer, the Carrizo and Upper Wilcox Aquifer, and the Lower Wilcox Aquifer.
- The two major shaly formations that restrict vertical groundwater flow are the Reklaw Formation and the Cook Mountain/Sparta/Weches Formation. Across most of the study area, there is more than 200 feet of shales associated with either formation.
- The Reklaw Formation is a thick shale formation that is easily traceable between logs and it serves as an effective hydrogeologic barrier to groundwater flow that hydraulically isolates the Queen City Aquifer above it from the Carrizo/Upper Wilcox Aquifer below it.
- The Cook Mountain/Sparta/Weches formation hydraulically isolates the Yegua-Jackson Aquifer above it from the Queen City Aquifer below it.
- The combination of the Tilden, Webb, and Yoakum Shales represent an effective barrier to groundwater flow between the Carrizo/Upper Wilcox Aquifer and the Lower Wilcox Aquifer.
- The Poth Shale is a good boundary marker for the base of the Wilcox Aquifer. Immediately below the Poth Shale the geophysical logs suggest that the deposits are shale rich for hundreds of feet.
- Fault zones occur in all dip cross-sections and are marked as a slanted line. Each of the fault zones produces an offset for all shale layers. The offsets associated with the faults are as large as 700 feet. Although represented by a slanted line, the offset associated with each fault zone, likely represents the total offset caused by a sequence of several faults.
- Despite large offsets with the faults, groundwater flows through the faults and remains in the same primary flow system on both sides of the fault. The continuity of the groundwater flow within a primary flow system as it passes through a fault is indicated by gradual and small changes in the water quality of

the groundwater across the faults within the same formation. The continuity of the flow system is most evident in the Carrizo/Upper Wilcox Aquifer. Across the up-dip fault locations in Figures 6 and 7 the groundwater with relatively low TDS concentrations in the Carrizo/Upper Wilcox Aquifer on the up-dip side of the fault does not mix with groundwater of much higher TDS concentrations in either the Queen City Aquifer or the Middle Wilcox Formation.

- The Carrizo/Upper Wilcox Aquifer contains freshwater at much greater depths than any formation. In Cross-Section F, freshwater occurs to depths approaching 4,000 feet and slightly saline groundwater occurs at depths near 6,000 feet.
- The water quality profiles indicate that the down-gradient migration of fresh and slightly saline in the Carrizo/Upper Wilcox is greater in the southwestern portion of the two counties than in the northeastern.

4.0 SUMMARY

The study analyzed 95 geophysical logs to create five cross-sections through Karnes and Wilson counties. The cross-sections include three dip cross-sections and two strike cross-sections. The cross-sections show the stratigraphic boundaries, shale layers, and different water quality classifications of groundwater in the sand layers for the Carrizo-Wilcox Aquifer, the Queen City Aquifer, the Sparta Aquifer, the Yegua-Jackson Aquifer, and the Gulf Coast Aquifer System. The stratigraphic boundaries for the Carrizo-Wilcox Aquifer are based on a chronostratigraphic framework based on the work of Hargis (1985, 1986, 2009, 2015a,b) and Hamlin (1988). The keystone to the mapping the stratigraphy of the Carrizo-Wilcox aquifer is the identification and mapping of ten major transgressive shales that are significant key markers and boundaries for delineating the Carrizo-Wilcox Aquifer. The names and abbreviation of these ten shales are the Reklaw, Hobson, Runge, Kenedy, Clayton, Dull, Yoakum, Webb, Tilden and Poth Shales. The stratigraphic boundaries between the major and minor aquifers that are younger than the Carrizo-Aquifer are based on information from previous publications.

For all 95 geophysical logs, the resistivity/induction and the spontaneous potential curves were analyzed in PETRA to identify a continuous sequence of sands and clays for each log above the base of the Carrizo-Wilcox Aquifer. PETRA is a commercial software widely used in the oil and gas industry to manage and analyze geophysical logs. A total of 3,527 sand intervals were identified. The lithologic analysis shows that two shaly formations that significantly restrict vertical groundwater flow at the regional scale are the Reklaw Formation and the Cook Mountain/Sparta/Weches Formation. The Reklaw formation is typically more than 200 feet thick, is easily traceable between logs, and serves as an effective hydrogeologic barrier to groundwater flow between the Queen City Aquifer above it and the Carrizo/Upper Wilcox Aquifer below it. In addition, the shales associated with the Cook Mountain were mapped and these shales isolate the Yegua-Jackson from aquifers below it. The shales identified by Hargis (2009) that exist within the Carrizo-Wilcox Aquifer shown good continuity between the logs and can be mapped across fault offsets. The combination of the Tilden, Webb, and Yoakum Shales in the Middle Wilcox represents an effective barrier to groundwater flow between the Carrizo/Upper Wilcox Aquifer and the Lower Wilcox Aquifer.

For each of the sand intervals identified on the geophysical logs, the TDS concentration of the groundwater was estimated based on the resistivity or the sand interval. The TDS concentrations calculated from the resistivity values was used to classify the water quality of the groundwater into the following classifications: fresh water (TDS concentration less than 1,000 mg/L), slightly saline (TDS concentration between 1,000 and 3,000 mg/L), moderately saline (TDS concentration between 3,000 and 10,000 mg/L), and very saline (TDS concentration above 10,000 mg/L). The TDS concentrations for the sand intervals was estimated using an approach called the Mean R_o Method, which involves calculating TDS from resistivity measurements on a geophysical log. The Mean R_o Method that has been applied in numerous studies in the Carrizo-Wilcox Aquifer and Gulf Coast Aquifer System. For this study, the resistivity values used to assign the TDS concentrations are aquifer-dependent and are based on previous studies published by the TWDB.

Faults were mapped in the three dip cross-sections. Despite offsets across the faults of up to 700 feet, groundwater appears to flow through the faults while primarily remaining in the same formation. The continuity of the groundwater flow through a fault within a single formation is indicated by gradual and small changes in the water quality within the different formations across a fault. The continuity in TDS concentrations across faults is most evident in the Carrizo/Upper Wilcox Aquifer, which is a smaller aquifer within the Carrizo-Wilcox Aquifer. The Carrizo/Upper Wilcox Aquifer also contains freshwater at much greater depths than any formation.

In the furthest southwest dip cross-section of the Carrizo/Upper Wilcox Aquifer, freshwater occurs to depths approaching 4,000 feet in the Carrizo-Wilcox Aquifer and slightly saline groundwater occurs at depths near 6,000 feet.

5.0 REFERENCES

Archie, G.E. 1942. The electrical resistivity log as an aid in determining some reservoir characteristics: Petroleum Transactions of AIME 146: 54–62.

Ayers, W.B. and A.H. Lewis. 1985. Systems and Deep-Basin Lignite: The University of Texas at Austin, Bureau of Economic Geology.

Collier, H. 1993. Borehole geophysical techniques for determining the water quality and reservoir parameters of fresh and saline water aquifers in Texas: Texas Water Development Board, Report 343, vol. I&II.

Deeds, N.E., T. Yan, A. Singh, T. Jones, V. Kelley, P. Knox, and S. Young. 2010. Groundwater Availability Model for the Yegua-Jackson Aquifer, Texas Water Development Board, GAM

Driscoll, F.G. 1986. Groundwater and Wells: St. Paul, MN, Johnson Filtration Systems, Inc., 1079 p.

Estepp, J. 1998. Evaluation of ground-water quality using geophysical logs: Texas Natural Resource Conservation Commission, unpublished Report, 516 p.

Estepp, J.D. 2010. Determining groundwater quality using geophysical logs: Texas Commission on Environmental Quality, unpublished report, 85 p.

Fogg, G.E. 1980. Geochemistry of ground water in the Wilcox aquifer, *in* Kreitler, C.W., Agagu, O.K., Basciano, J.M., Collins, E.W., Dix, O., Dutton, S.P., Fogg, G.E., Giles, A.B., Guevara, E.H., Harris, D.W., Hobday, D.K., McGowen, M.K., Pass, D. and Wood, D.H., 1979, Geology and Geohydrology of the East Texas Basin A Report on the Progress of Nuclear Waste Isolation Feasibility Studies: The University of Texas at Austin, Bureau of Economic Geology (1979), Geologic Circular No. 80-12, p. 73-78.

Fogg, G.E., and P.E. Blanchard. 1986. Empirical relations between Wilcox groundwater quality and electric log resistivity, Sabine Uplift area, *in* Kaiser, W.R. ed., Geology and Groundwater hydrology of deep-basin lignite in the Wilcox Group of East Texas: The University of Texas at Austin, Bureau of Economic Geology, Special Report No. 10, p. 115-118.

Fogg, G.E. and C.W. Kreitler. 1982. Ground-water hydraulics and hydrochemical facies in eocene aquifers of the East Texas Basin. The University of Texas at Austin, Bureau of Economic Geology, Report of Investigations No. 127, 75 p

Hamlin, H.S. 1988. Depositional and ground-water flow systems of the Carrizo-Upper Wilcox, South Texas: The University of Texas at Austin, Bureau of Economic Geology, Report of Investigations No. 175

Hamlin, H. and L. de la Rocha. 2015, Using electric logs to estimate groundwater salinity and map brackish groundwater resources in the Carrizo-Wilcox Aquifer in South Texas: GCAGS Journal v.4 (2015), p. 109-131.

Hamlin, H.S., D.A. Smith, and M.S. Akhter. 1988. Hydrogeology of Barbers Hill salt dome, Texas coastal plain: The University of Texas at Austin, Bureau of Economic Geology, Report of Investigations No. 176, 41 p.

Hamlin, S., B.R. Scanlon, R. Reedy, S.C. Young, and M. Jigmond. 2016. Fresh, Brackish, and Saline Groundwater in the Carrizo-Wilcox Aquifer in Groundwater Management Area 13 -- Location, Quantification, Producibility, and Impacts

Hargis, R. N. 1985. Proposed lithostratigraphic classification of the Wilcox Group of South Texas: Gulf Coast Association of Geological Societies Transactions, v. 35, p. 107–159.

Hargis, R. N. 1986. Proposed Stratigraphic Classification of the Wilcox of South Texas: Contributions to the Geology of South Texas, 1986, South Texas Geological Society, p.135-159.

Hargis, R. N. 2009. Major Transgressive Shales of the Wilcox, Northern Portion of South Texas, South Texas Geological Society Bulletin, April 2009, p. 19-47.

Hargis, R. N. 2015a. Report on Study of Wilcox Group Northern Atascosa County and Adjacent Areas of Bexar and Wilson Counties, prepared for the Evergreen Underwater Conservation District, Pleasanton, TX

Hargis, R. N. 2015b. Report on Study of Wilcox Group Wilson County Study Area and Adjacent Areas of Bexar and Wilson Counties, prepared for the Evergreen Underwater Conservation District, Pleasanton, TX

IHS. 2009. User's Manual for PETRA. Information Handling Services, Houston, TX.

Kelley, V.A., N.E. Deeds, D.G. Fryar, and J-P Nicot. 2004. Groundwater Availability Models for the Queen City and Sparta Aquifers: prepared for the Texas Water Development Board.

Lupton, D., V. Kelley, D. Powers, and C. Torres-Verdin. 2016. Identification of Potential Brackish Groundwater Production Areas – Rustler Aquifer. Prepared for the Texas Water Development Board, Austin, TX

Meyer, J.E. 2012. Geologic characterization of and data collection in the Corpus Christi Aquifer Storage and Recovery Conservation District and surrounding counties: Texas Water Development Board, Austin, TX, Open File Report 12-01.

Meyer, J.E., A. Croskrey, M.R. Wise, and S. Kalaswad. 2014. Brackish Groundwater in the Gulf Coast Aquifer, Lower Rio Grande Valley, Texas: Texas Water Development Board Report 383, 107 p.

Winslow, A.G., and L.R. Kister. 1956. Saline-water resources of Texas: U.S. Geological Survey Water-Supply Paper 1365, 105 p.

Wise, M, R. 2014. Queen City and Sparta Aquifers, Atascosa and McMullen Counties, Texas: Structure and Brackish Groundwater. Technical note 14-01. Texas Water Development Board, Austin TX

Young, S. C. and V. Kelley, editors. 2006. A site conceptual model to support the development of a detailed groundwater model for Colorado, Wharton, and Matagorda counties, prepared for the Lower Colorado River Authority, Austin, TX.

Young, S.C. and D. Lupton. 2014. Gulf Coast Aquifer System groundwater study for the City of Corpus Christi: Phase 1. Prepared for the City of Corpus Christi, Corpus Christi, TX. April 2014.

Young, S.C., V. Kelley, T. Budge, N. Deeds, and P. Knox. 2009. Development of the LCRB Groundwater Flow Model for the Chicot and Evangeline aquifers in Colorado, Wharton, and Matagorda counties: LSWP Report Prepared by the URS Corporation, prepared for the Lower Colorado River Authority, Austin, TX.

Young, S., T. Budge, P. Knox, R. Kalbouss, E. Baker, S. Hamlin, B. Galloway, and N. Deeds. 2010. Final hydrostratigraphy of the Gulf Coast Aquifer System from the Brazos River to the Rio Grande, (Final Report): Texas Water Development Board, 203p.

Young, S., T. Ewing, S. Hamlin, E. Baker, and D. Lupton. 2012. Final Report updating the hydrogeologic framework for the Northern Portion of the Gulf Coast Aquifer System. Prepared for the Texas Water Development Board, June 2012.Young and others (2013).

Young, S. C., M. Jigmond, N. Deeds, J. Blainey, T.E. Ewing, and D. Banerji. 2016. Final Report Identification of Potential Brackish Groundwater Production Areas – Gulf Coast Aquifer System., prepared for the Texas Water Development Board, Austin, TX.

FIGURES

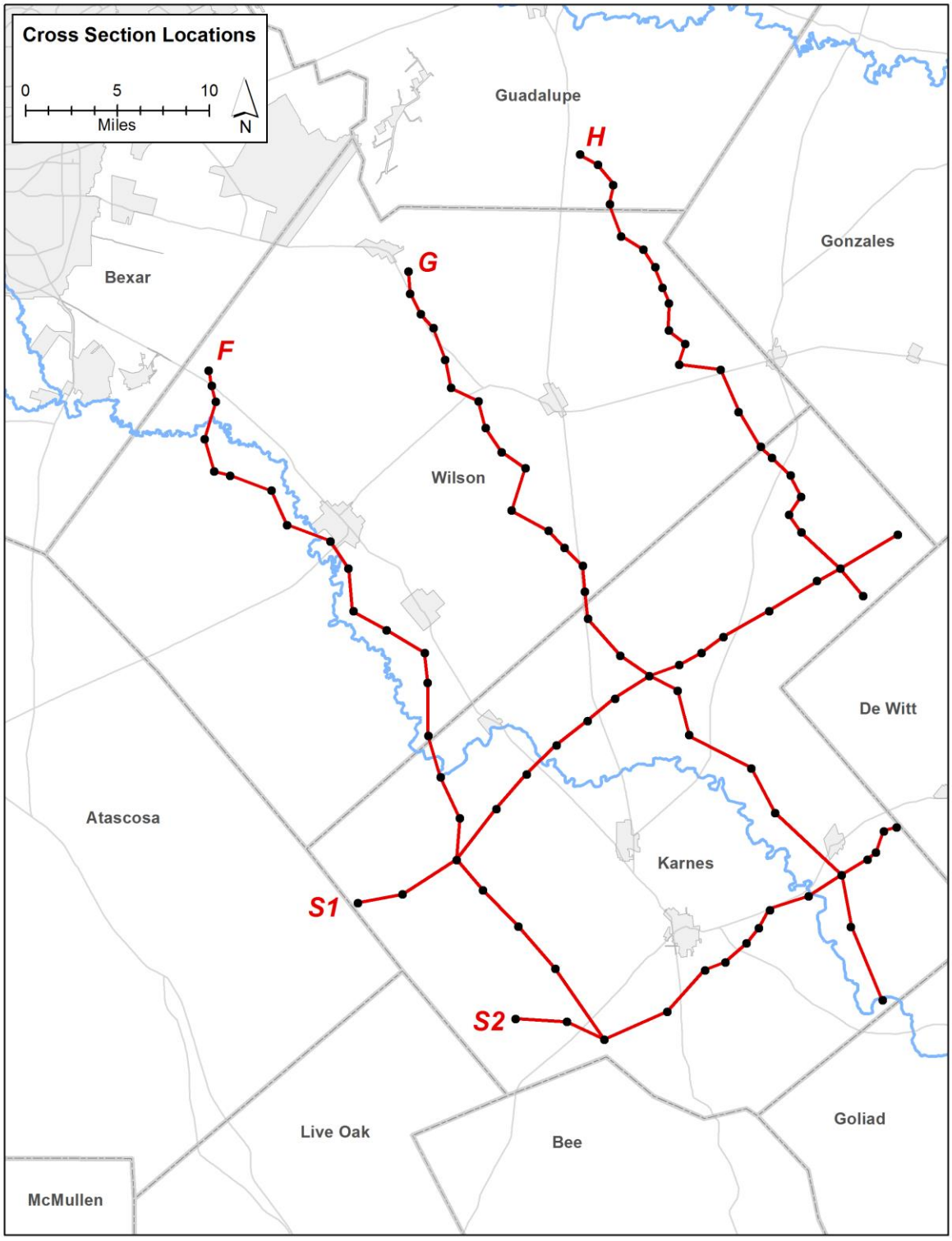

Figure 1 Location of 95 geophysical logs used to construct Dip Sections F, G, and H and Strike Sections S1 and S2 in Wilson and Karnes Counties

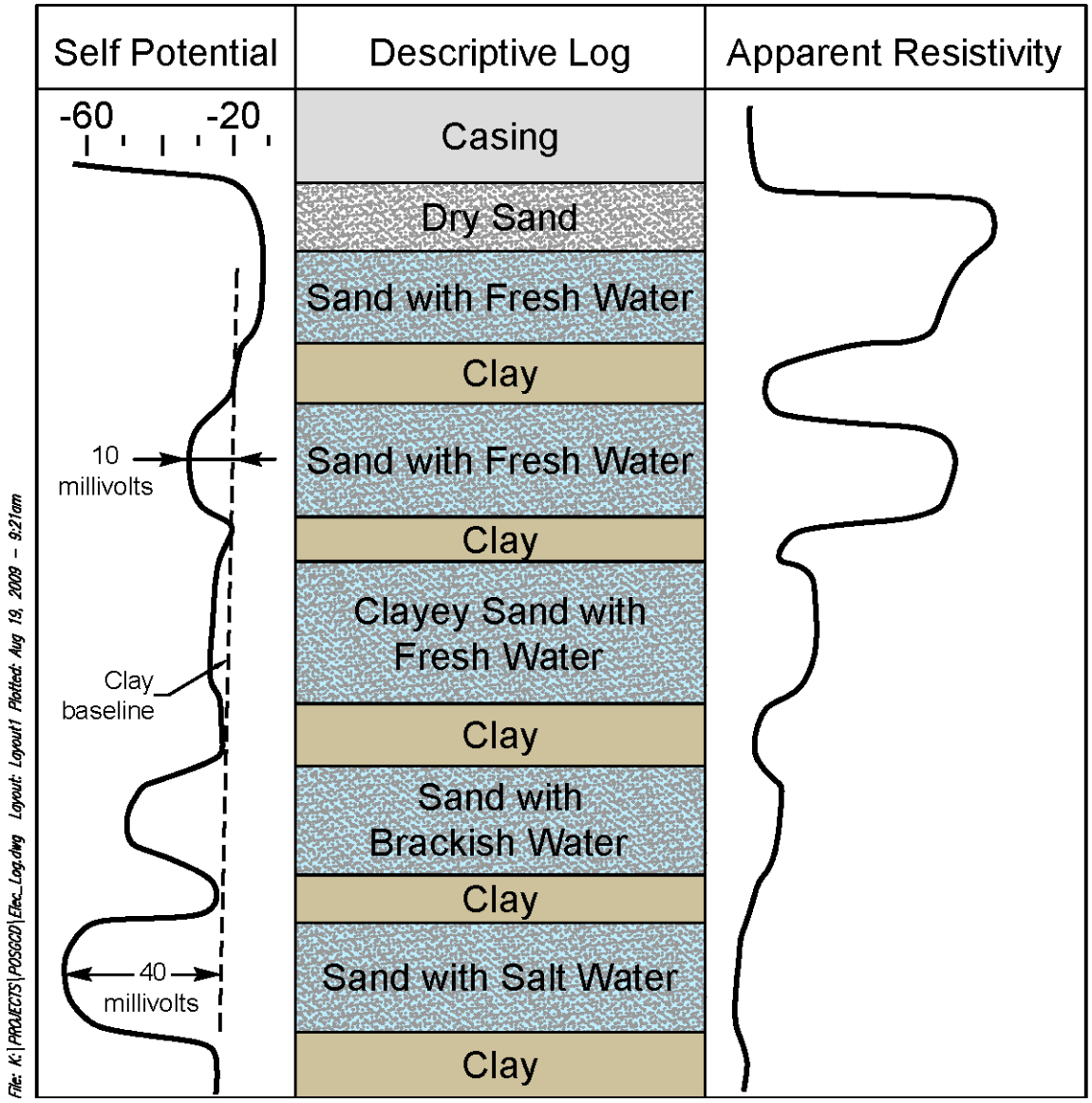

Figure 2 Idealized SP and resistivity curve showing the responses corresponding to alternating sand and clay strata that are saturated with groundwater which increases significantly in TDS concentrations with depth. Modified from Driscoll (1986, p. 189).

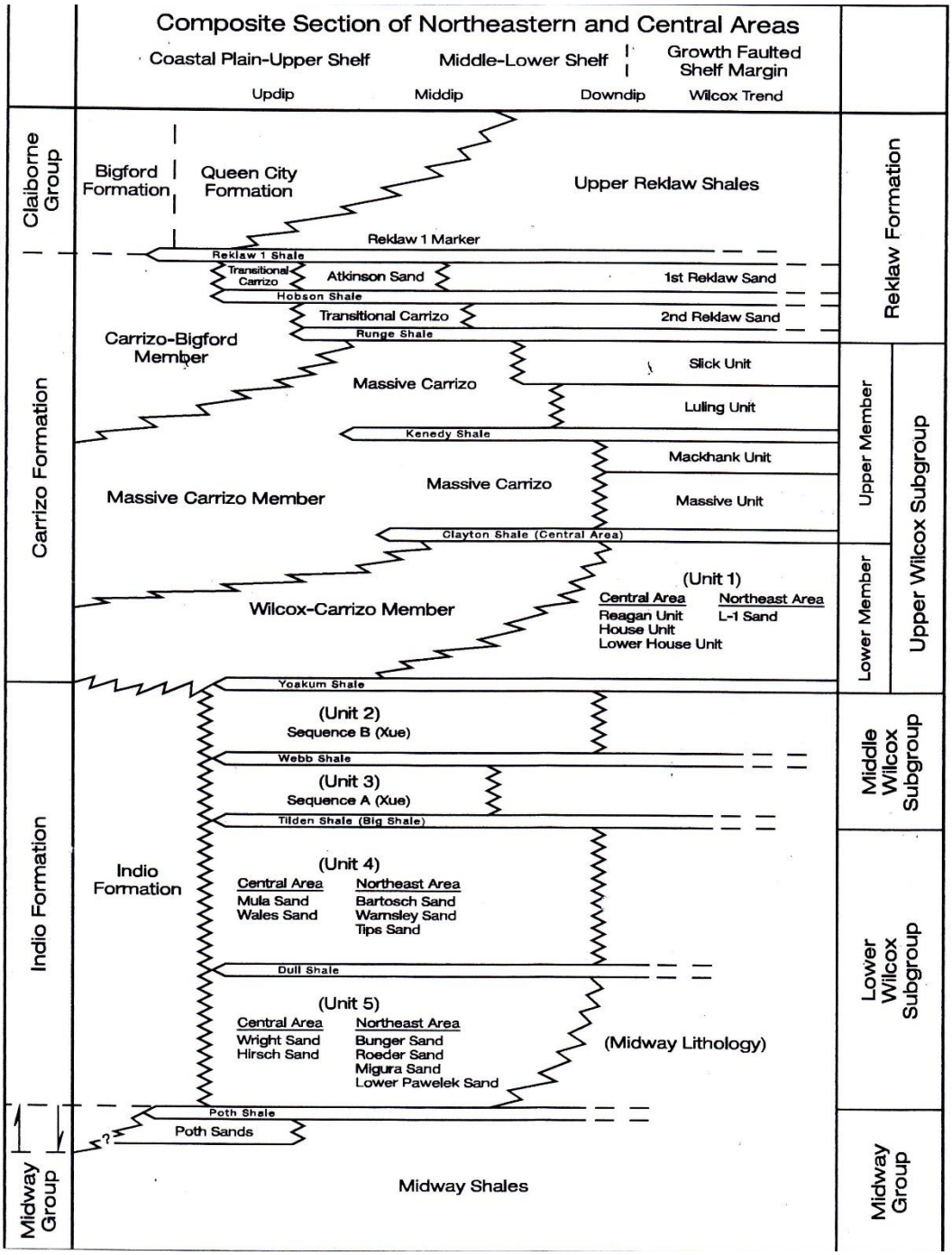

Figure 3 Classification of Wilcox Group including the stratigraphic position of ten major transgressive shales used by Hargis (2009). (Figure taken from Hargis [2015a].)

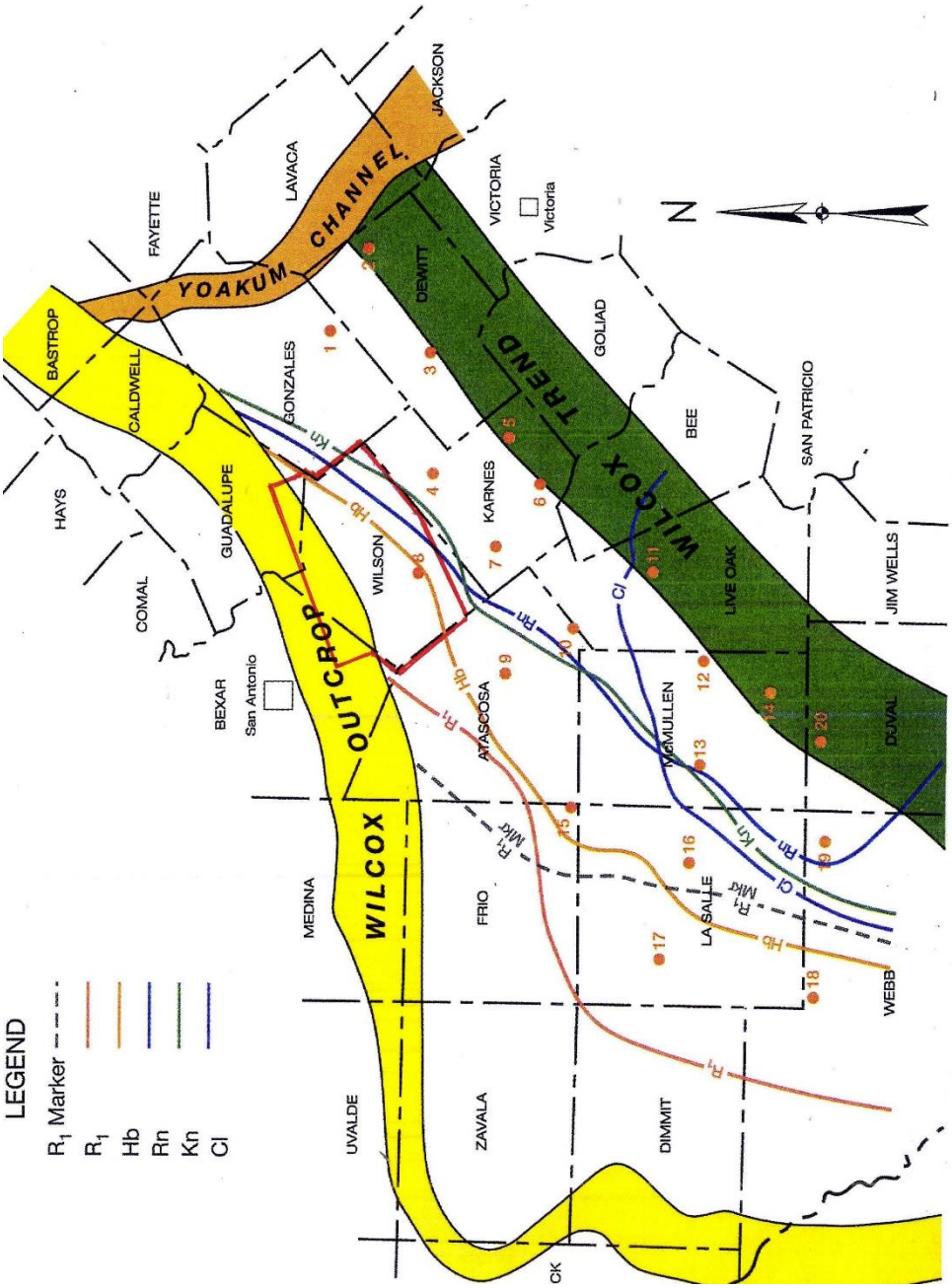

Figure 4 Approximate regional limits of Reklaw Shale (R1), Hobson Shale (Hb), Runge Shale (Rn), and Kenedy Shale (Kn) in the vicinity of Evergreen Underground Water Conservation District. (Figure copied from Hargis [2015b].)

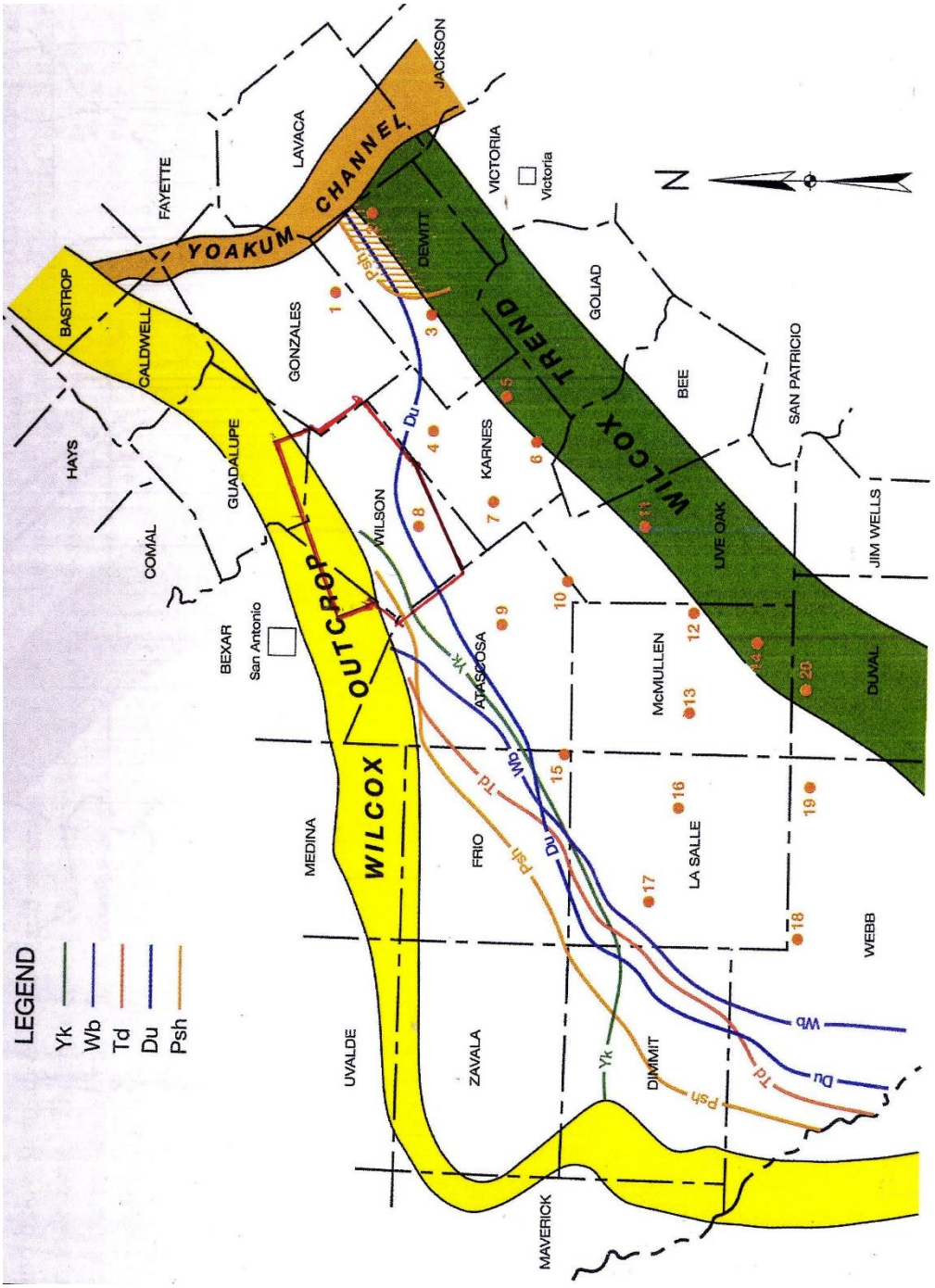

Figure 5 Approximate regional limits of Yoakum Shale (Yk), Webb Shale (Wb), Tilden Shale (Td), Dull Shale (Du) and Poth Shale (Psh) in the vicinity of Evergreen Underground Water Conservation District. (Figure copied from Hargis [2015b].)

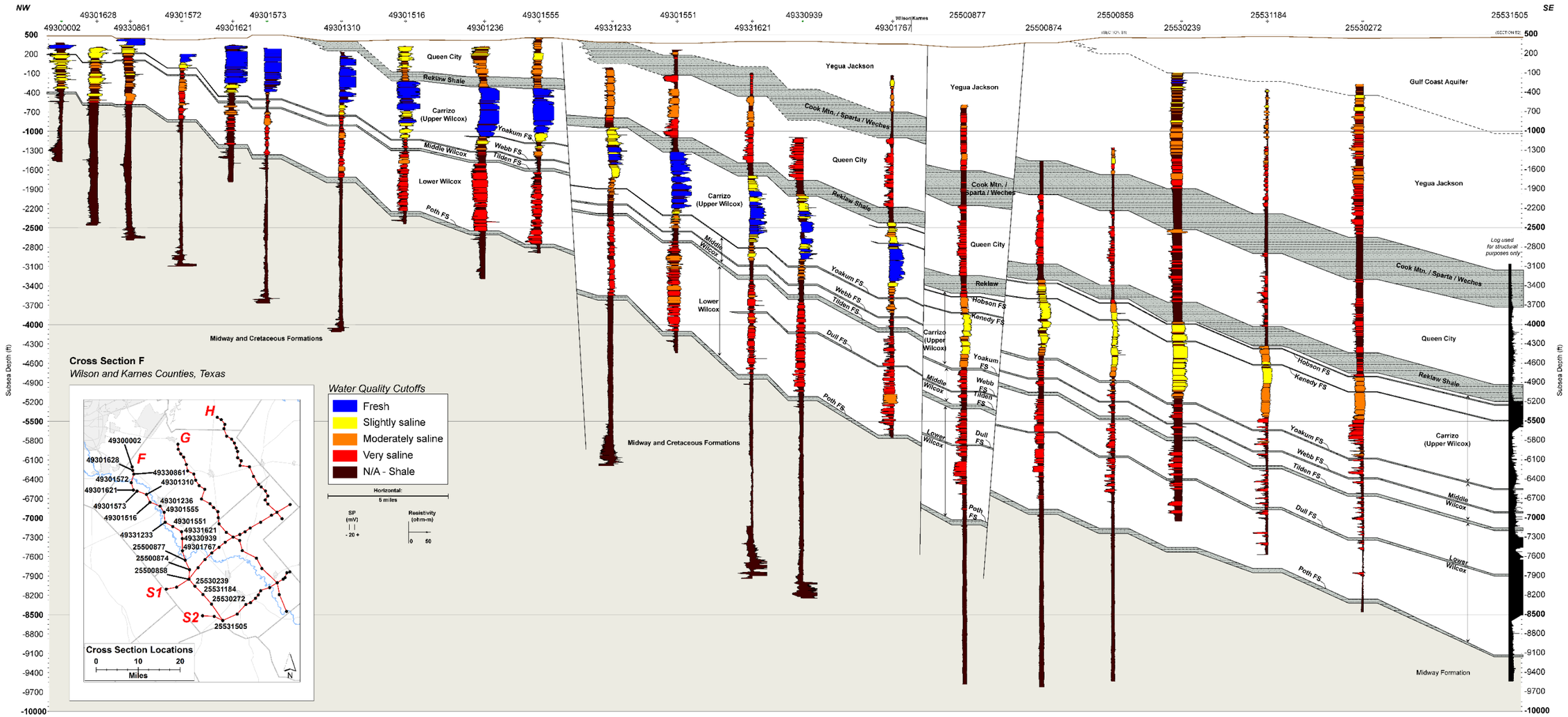

Figure 6 Dip cross-section F showing stratigraphy, shale locations, sand intervals, and water quality classifications at 22 log locations

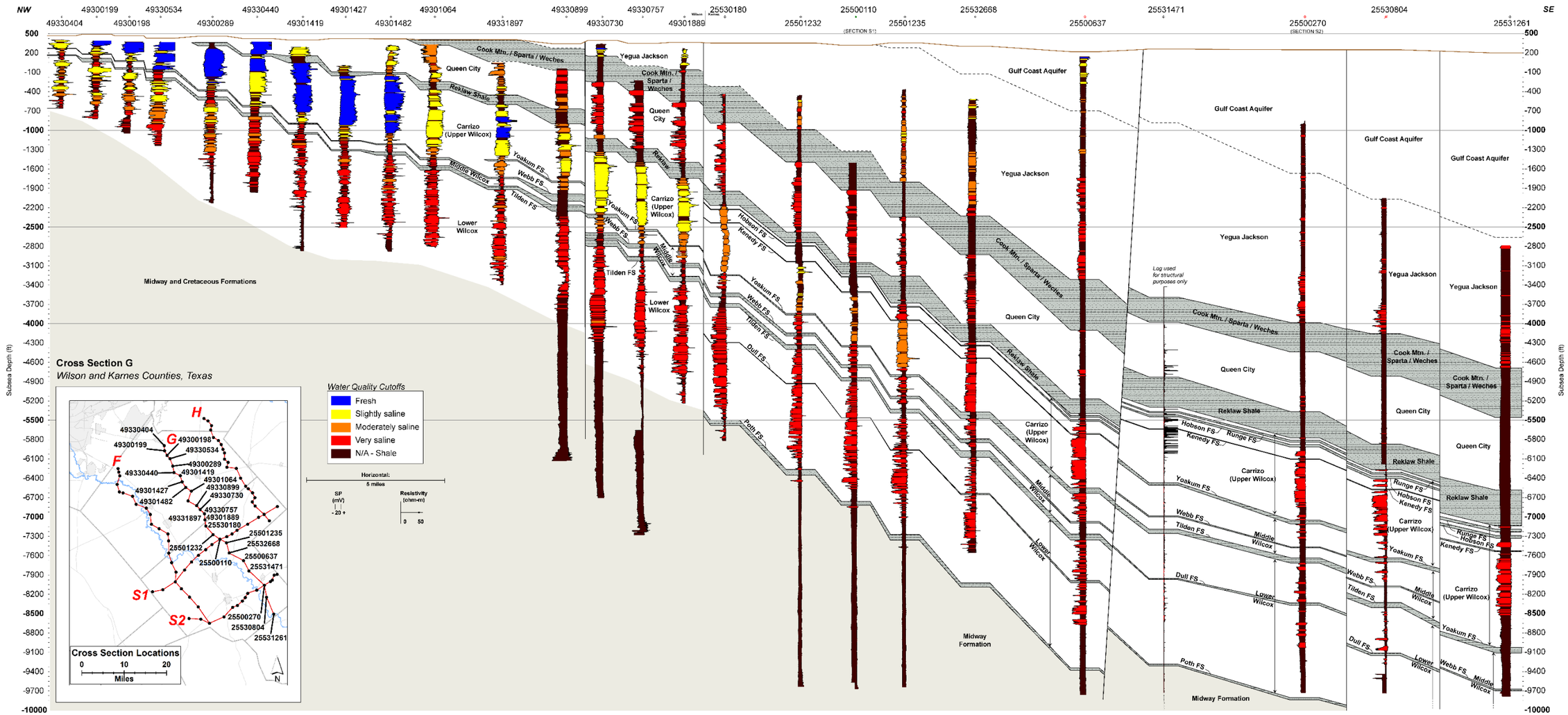

Figure 7 Dip cross-section G showing stratigraphy, shale locations, sand intervals, and water quality classifications at 25 log locations

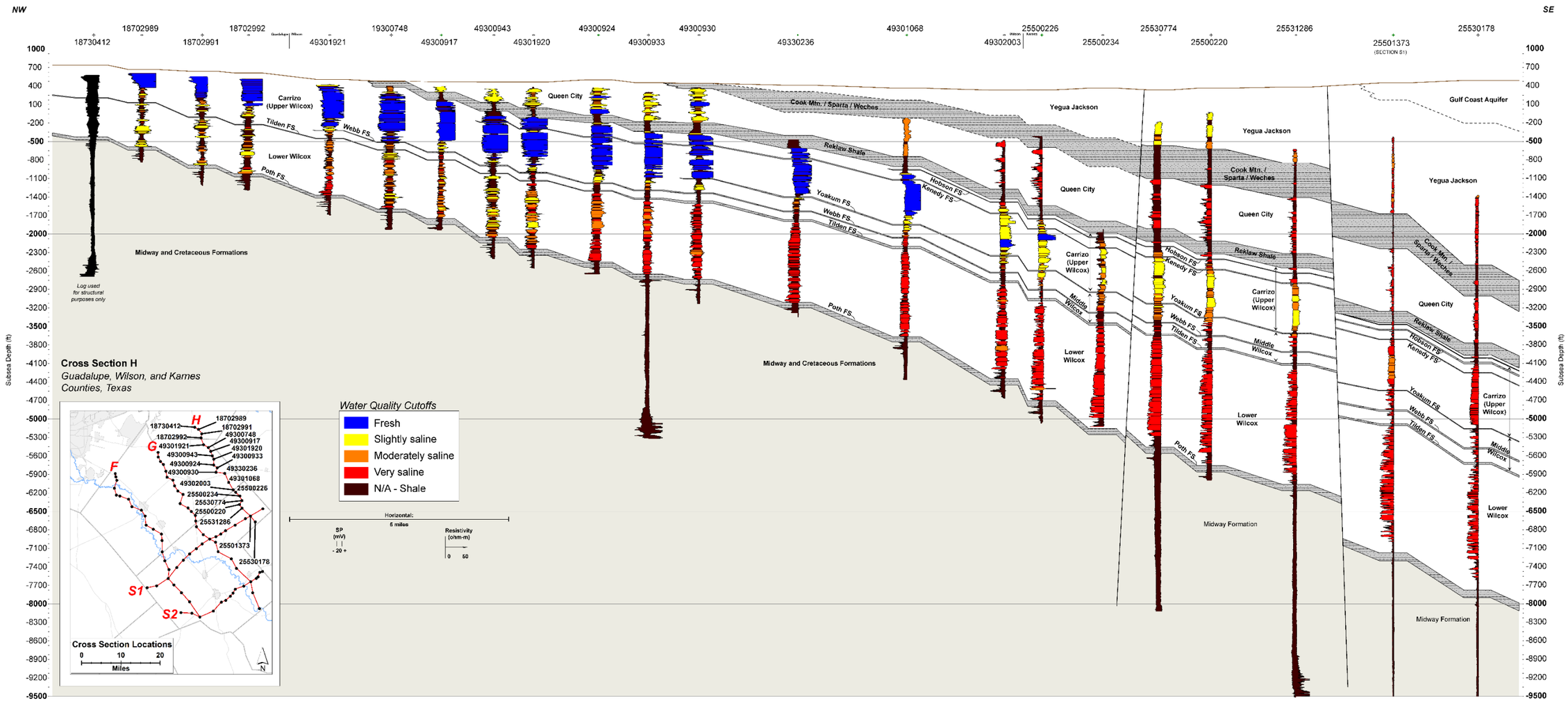

Figure 8 Dip cross-section H showing stratigraphy, shale locations, sand intervals, and water quality classifications at 22 log locations

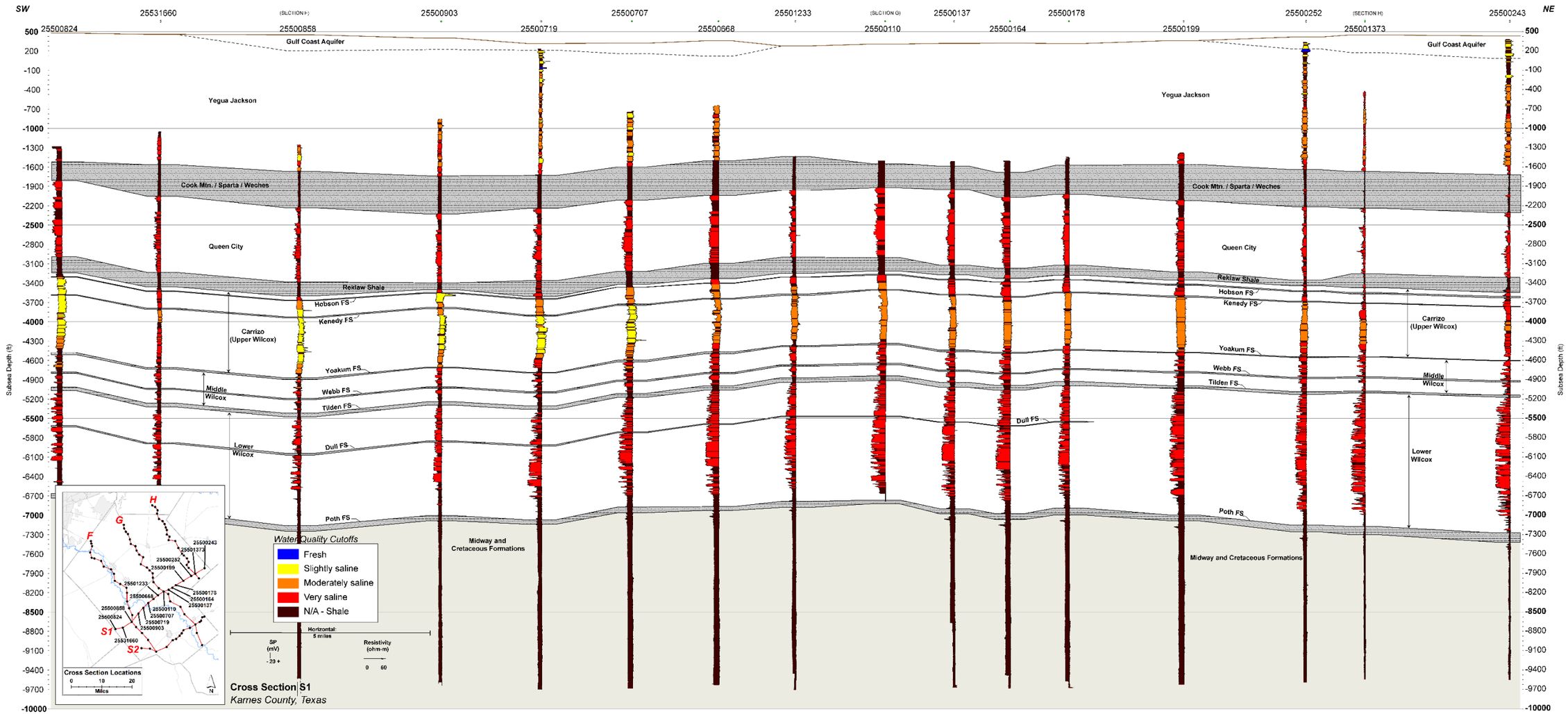

Figure 9 Strike cross-section S1 showing stratigraphy, shale locations, sand intervals, and water quality classifications at 16 log locations

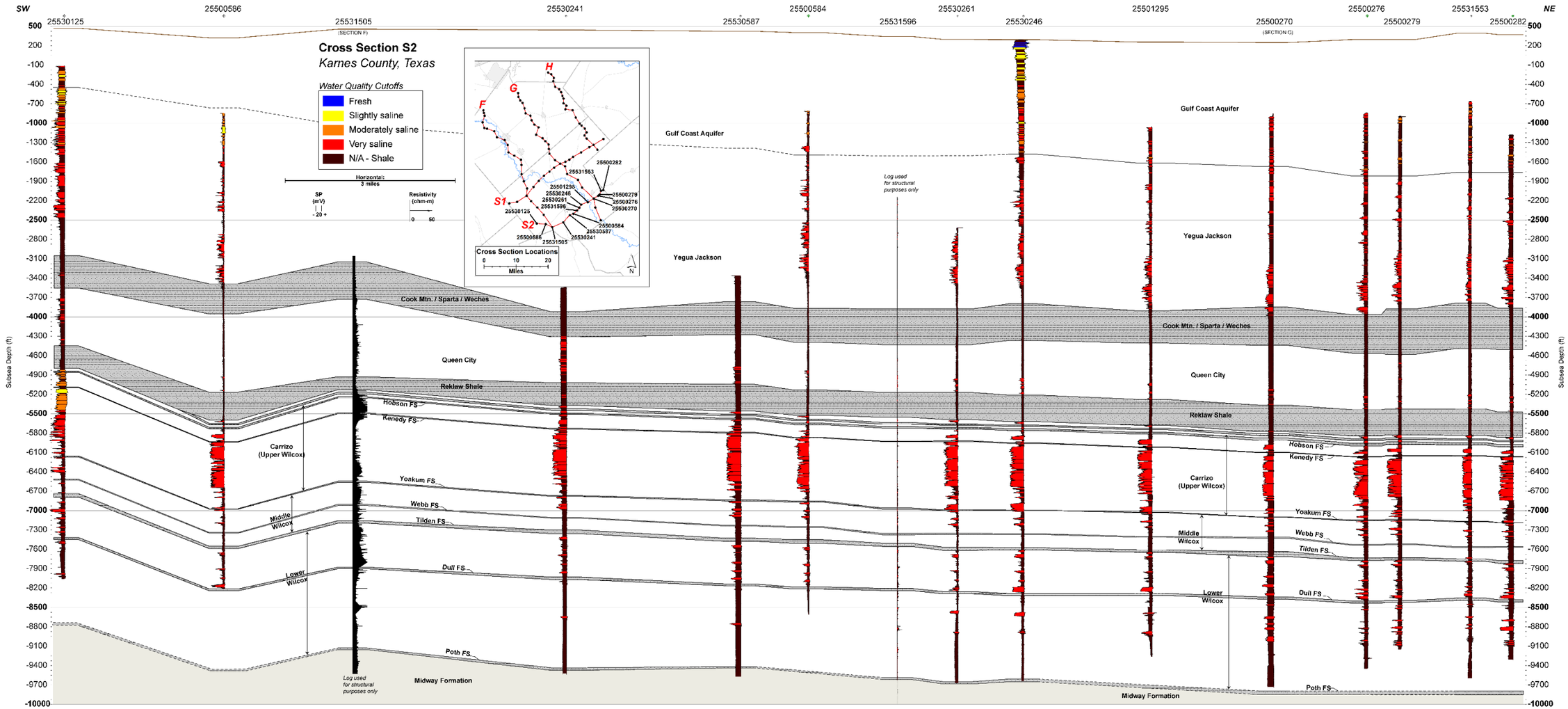

Figure 10 Strike cross-section S2 showing stratigraphy, shale locations, sand intervals, and water quality classifications at 15 log locations

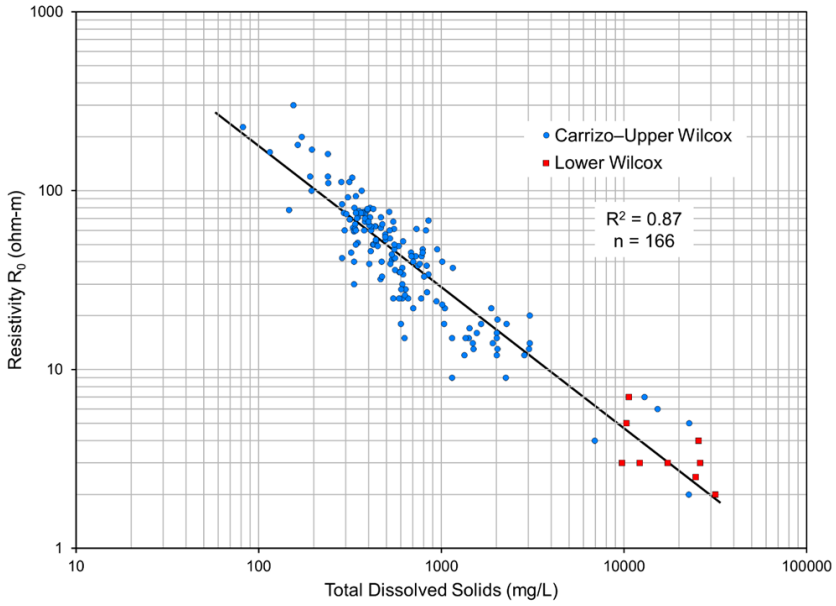

Figure 11 R_0 versus TDS concentration or the Carrizo-Upper Wilcox Aquifer in GAM 13 based on analysis of geophysical logs that are located near wells with measured TDS concentrations. (Figure copied from Hamlin and others [2016].)

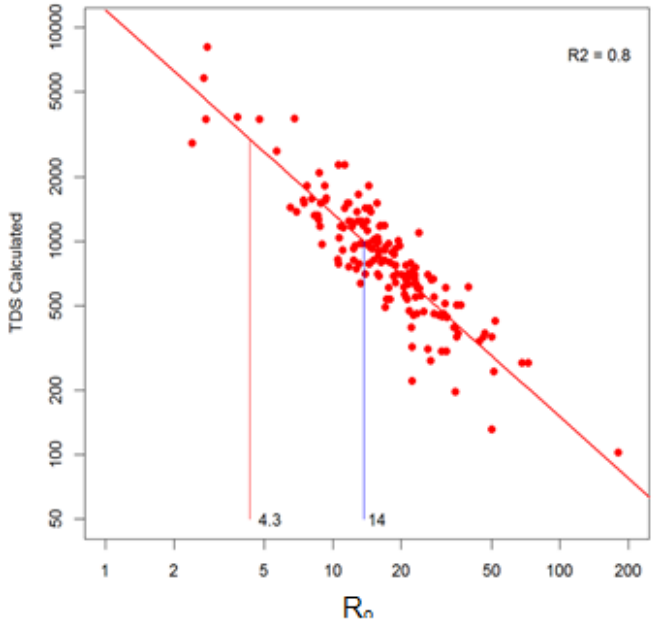

Figure 12 TDS concentration versus R_0 for the Chicot Aquifer in the Gulf Coast Aquifer System based on analysis of geophysical logs that are located near wells with measured TDS concentrations. (Figure copied from Young and others [2016].)

APPENDIX: GEOPHYSICAL WELL LOG INFORMATION

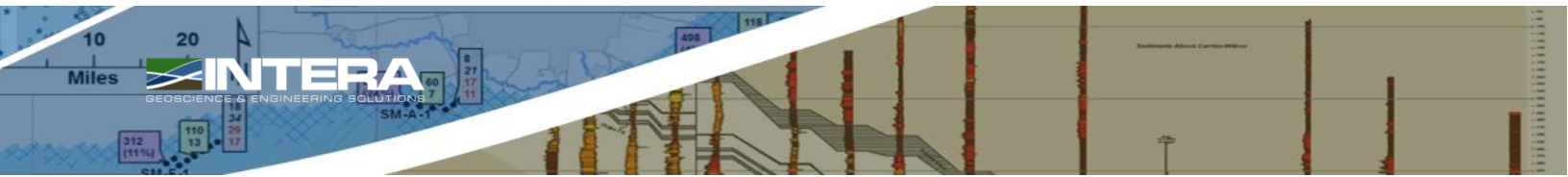

Table A-1 Location of the geophysical logs

API ID	Latitude (NAD 88)	Longitude (NAD 88)	County	Dip Section / Position	Strike Section / Position	Number of Sand Picks
4225500137	29.025821	-97.851176	Karnes	-	1-10	9
4225500164	29.035287	-97.830883	Karnes	-	1-11	19
4225500178	29.047815	-97.811158	Karnes	-	1-12	8
4225500199	29.067967	-97.76979	Karnes	-	1-13	22
4225500243	29.12762	-97.653729	Karnes	-	1-16	47
4225500252	29.091439	-97.726929	Karnes	-	1-14	58
4225500276	28.871273	-97.683161	Karnes	-	2-12	53
4225500279	28.8767	-97.675584	Karnes	-	2-13	39
4225500282	28.896577	-97.656899	Karnes	-	2-15	37
4225500584	28.790988	-97.811492	Karnes	-	2-06	35
4225500586	28.744752	-97.953727	Karnes	-	2-01	40
4225500668	28.98202	-97.933515	Karnes	-	1-07	24
4225500707	28.96294	-97.961812	Karnes	-	1-06	21
4225500719	28.940006	-97.98853	Karnes	-	1-05	57
4225500824	28.839114	-98.140573	Karnes	-	1-01	14
4225500903	28.912778	-98.015774	Karnes	-	1-04	27
4225501233	28.999555	-97.908905	Karnes	-	1-08	7
4225501295	28.842642	-97.736271	Karnes	-	2-10	51
4225530125	28.747225	-97.999674	Karnes	-	2-02	60
4225530241	28.752064	-97.863852	Karnes	-	2-04	83
4225530246	28.831933	-97.771218	Karnes	-	2-09	83
4225530261	28.817593	-97.781037	Karnes	-	2-08	22
4225530587	28.784665	-97.829734	Karnes	-	2-05	6
4225531553	28.893337	-97.66834	Karnes	-	2-14	44
4225531596	28.805733	-97.792235	Karnes	-	2-07	19
4225531660	28.845982	-98.100508	Karnes	-	1-02	34
4249300002	29.260047	-98.273293	Wilson	F-01	-	17
4249301628	29.248036	-98.270634	Wilson	F-02	-	16
4249330861	29.23554	-98.266885	Wilson	F-03	-	19
4249301572	29.205937	-98.277171	Wilson	F-04	-	23
4249301621	29.180363	-98.268619	Wilson	F-05	-	21
4249301573	29.176967	-98.254295	Wilson	F-06	-	29
4249301310	29.165154	-98.217092	Wilson	F-07	-	1
4249301516	29.137859	-98.203254	Wilson	F-08	-	13
4249301236	29.124706	-98.16402	Wilson	F-09	-	15
4249301555	29.103384	-98.147971	Wilson	F-10	-	18
4249331233	29.069611	-98.1437	Wilson	F-11	-	13

API ID	Latitude (NAD 88)	Longitude (NAD 88)	County	Dip Section / Position	Strike Section / Position	Number of Sand Picks
4249301551	29.054439	-98.114059	Wilson	F-12	-	10
4249331621	29.036347	-98.079875	Wilson	F-13	-	21
4249330939	29.012976	-98.077341	Wilson	F-14	-	15
4249301767	28.971029	-98.076953	Wilson	F-15	-	20
4225500877	28.938294	-98.065925	Karnes	F-16	-	46
4225500874	28.905701	-98.048995	Karnes	F-17	-	16
4225500858	28.87273	-98.051893	Karnes	F-18	1-03	29
4225530239	28.848835	-98.028464	Karnes	F-19	-	49
4225531184	28.820121	-97.996849	Karnes	F-20	-	41
4225530272	28.786644	-97.963694	Karnes	F-21	-	75
4225531505	28.730428	-97.920331	Karnes	F-22	2-03	61
4249330404	29.337299	-98.090471	Wilson	G-01	-	28
4249300199	29.319487	-98.091171	Wilson	G-02	-	31
4249300198	29.304872	-98.082109	Wilson	G-03	-	33
4249330534	29.292792	-98.070259	Wilson	G-04	-	29
4249300289	29.267983	-98.059734	Wilson	G-05	-	40
4249330440	29.245544	-98.055473	Wilson	G-06	-	30
4249301419	29.234478	-98.032011	Wilson	G-07	-	43
4249301427	29.216927	-98.017193	Wilson	G-08	-	45
4249301482	29.194951	-98.00953	Wilson	G-09	-	75
4249301064	29.181557	-97.989057	Wilson	G-10	-	50
4249331897	29.148453	-98.000119	Wilson	G-11	-	71
4249330899	29.132391	-97.967835	Wilson	G-12	-	40
4249330730	29.118876	-97.953748	Wilson	G-13	-	69
4249330757	29.104575	-97.936986	Wilson	G-14	-	57
4249301889	29.083288	-97.935866	Wilson	G-15	-	98
4225530180	29.062825	-97.932801	Karnes	G-16	-	117
4225501232	29.033543	-97.904142	Karnes	G-17	-	93
4225500110	29.017369	-97.877952	Karnes	G-18	1-09	81
4225501235	29.005645	-97.852811	Karnes	G-19	-	111
4225532668	28.970514	-97.842393	Karnes	G-20	-	103
4225500637	28.943994	-97.786869	Karnes	G-21	-	85
4225531471	28.908472	-97.765903	Karnes	G-22	-	0
4225500270	28.85892	-97.706405	Karnes	G-23	2-11	96
4225530804	28.818178	-97.698851	Karnes	G-24	-	51
4225531261	28.760003	-97.670824	Karnes	G-25	-	33
4218730412	29.429515	-97.937575	Guadalupe	H-01	-	20
4218702989	29.421551	-97.921798	Guadalupe	H-02	-	16

API ID	Latitude (NAD 88)	Longitude (NAD 88)	County	Dip Section / Position	Strike Section / Position	Number of Sand Picks
4218702991	29.405394	-97.908158	Guadalupe	H-03	-	20
4218702992	29.390264	-97.911164	Guadalupe	H-04	-	25
4249301921	29.364771	-97.901138	Wilson	H-05	-	30
4249300748	29.354074	-97.88129	Wilson	H-06	-	3
4249300917	29.340358	-97.870584	Wilson	H-07	-	1
4249300943	29.323846	-97.864063	Wilson	H-08	-	1
4249301920	29.311643	-97.858435	Wilson	H-09	-	9
4249300924	29.290086	-97.858562	Wilson	H-10	-	56
4249300933	29.279403	-97.84409	Wilson	H-11	-	51
4249300930	29.26324	-97.849321	Wilson	H-12	-	63
4249330236	29.258718	-97.81232	Wilson	H-13	-	48
4249301068	29.225431	-97.796133	Wilson	H-14	-	2
4249302003	29.197954	-97.776539	Wilson	H-15	-	5
4225500226	29.18913	-97.766533	Karnes	H-16	-	11
4225500234	29.175159	-97.749828	Karnes	H-17	-	43
4225530774	29.157957	-97.74058	Karnes	H-18	-	10
4225500220	29.143922	-97.751331	Karnes	H-19	-	16
4225531286	29.130138	-97.740439	Karnes	H-20	-	24
4225501373	29.101196	-97.705389	Karnes	H-21	1-15	46
4225530178	29.079267	-97.685422	Karnes	H-22	-	31

Table A-2 Depth (feet) to aquifers and formations

API ID	Datum	Dip Section/ Position	Strike Section/ Position	Number of Sand Picks	GMA 13 BRACS Study	Hargis Study	Depth (Feet) to Top of Aquifers and Formations					
							Yegua Jackson Top	Cook Mountain / Sparta / Weches Top	Queen City Top	Carrizo / Upper Wilcox Top	Middle Wilcox Top	Lower Wilcox Top
4225500137	329	-	1-10	9	No	No	16	1,915	2,279	-	-	-
4225500164	314	-	1-11	19	Yes	No	0	1,994	2,379	3,699	4,734	5,436
4225500178	324	-	1-12	8	No	No	9	1,897	2,347	-	-	-
4225500199	377	-	1-13	22	Yes	No	16	1,936	2,498	3,811	4,780	5,470
4225500243	450	-	1-16	47	Yes	No	368	2,166	2,756	4,078	4,993	5,689
4225500252	408	-	1-14	58	Yes	No	176	2,047	2,619	3,979	4,898	5,596
4225500276	301	-	2-12	53	No	No	2,121	4,268	4,864	-	-	-
4225500279	319	-	2-13	39	No	No	2,139	4,197	4,900	-	-	-
4225500282	370	-	2-15	37	No	No	2,134	4,235	4,876	-	-	-
4225500584	419	-	2-06	35	No	No	1,909	4,285	4,813	-	-	-
4225500586	336	-	2-01	40	No	No	1,098	3,823	4,290	-	-	-
4225500668	370	-	1-07	24	Yes	No	249	1,873	2,410	3,774	4,793	5,490
4225500707	316	-	1-06	21	No	No	156	1,913	2,426	-	-	-
4225500719	299	-	1-05	57	Yes	No	86	2,029	2,538	3,952	5,016	5,710
4225500824	496	-	1-01	14	Yes	No	19	2,013	2,303	3,807	4,913	5,673
4225500903	409	-	1-04	27	No	No	187	2,146	2,736	-	-	-
4225501233	295	-	1-08	7	Yes	No	19	1,734	2,255	3,113	4,172	4,829
4225501295	270	-	2-10	51	No	No	1,886	4,174	4,676	-	-	-
4225530125	491	-	2-02	60	No	No	938	3,539	4,045	-	-	-
4225530241	479	-	2-04	83	Yes	No	1,757	4,401	4,790	2,597	3,565	4,197

API ID	Datum	Dip Section/ Position	Strike Section/ Position	Number of Sand Picks	GMA 13 BRACS Study	Hargis Study	Depth (Feet) to Top of Aquifers and Formations					
							Yegua Jackson Top	Cook Mountain / Sparta / Weches Top	Queen City Top	Carrizo / Upper Wilcox Top	Middle Wilcox Top	Lower Wilcox Top
4225530246	361	-	2-09	83	Yes	No	1,842	4,159	4,728	4,451	5,597	6,321
4225530261	332	-	2-08	22	No	No	1,835	4,210	4,763	-	-	-
4225530587	431	-	2-05	6	No	No	1,818	4,195	4,706	-	-	-
4225531553	405	-	2-14	44	Yes	No	2,169	4,192	4,895	5,720	6,710	7,603
4225531596	375	-	2-07	19	No	No	1,883	4,253	4,806	-	-	-
4225531660	479	-	1-02	34	Yes	No	21	2,041	2,530	6,391	7,417	8,251
4249300002	473	F-01	-	17	No	No	-	-	-	-	-	-
4249301628	480	F-02	-	16	No	No	-	-	-	-	-	-
4249330861	567	F-03	-	19	No	No	-	-	-	-	-	-
4249301572	416	F-04	-	23	No	No	-	-	-	-	-	-
4249301621	431	F-05	-	21	No	No	-	-	-	-	-	-
4249301573	503	F-06	-	29	Yes	No	-	-	-	115	891	1,169
4249301310	427	F-07	-	1	Yes	No	-	-	-	305	1,072	1,358
4249301516	412	F-08	-	13	No	No	-	-	-	-	-	-
4249301236	419	F-09	-	15	No	No	-	-	10	-	-	-
4249301555	548	F-10	-	18	Yes	No	-	-	159	887	1,729	2,186
4249331233	388	F-11	-	13	No	No	-	11	335	-	-	-
4249301551	371	F-12	-	10	Yes	No	-	185	503	1,690	2,649	3,135
4249331621	409	F-13	-	21	No	No	-	402	867	-	-	-
4249330939	423	F-14	-	15	Yes	No	-	766	1,251	2,403	3,477	4,082
4249301767	359	F-15	-	20	Yes	No	-	1,056	1,461	2,858	3,894	4,536

API ID	Datum	Dip Section/ Position	Strike Section/ Position	Number of Sand Picks	GMA 13 BRACS Study	Hargis Study	Depth (Feet) to Top of Aquifers and Formations					
							Yegua Jackson Top	Cook Mountain / Sparta / Weches Top	Queen City Top	Carrizo / Upper Wilcox Top	Middle Wilcox Top	Lower Wilcox Top
4225500877	421	F-16	-	46	Yes	No	-	2,028	2,569	3,997	5,084	5,782
4225500874	379	F-17	-	16	Yes	No	5	1,833	2,361	3,752	4,861	5,531
4225500858	470	F-18	1-03	29	Yes	No	265	2,137	2,700	4,143	5,289	5,998
4225530239	451	F-19	-	49	Yes	No	543	2,340	2,975	4,589	5,580	6,292
4225531184	489	F-20	-	41	No	No	716	2,764	3,385	-	-	-
4225530272	450	F-21	-	75	Yes	No	890	3,093	3,747	6,117	7,183	8,029
4225531505	472	F-22	2-03	61	Yes	No	1,504	3,622	4,200	3,030	3,957	4,589
4249330404	470	G-01	-	28	No	No	-	-	-	-	-	-
4249300199	491	G-02	-	31	No	No	-	-	-	-	-	-
4249300198	468	G-03	-	33	No	No	-	-	-	-	-	-
4249330534	430	G-04	-	29	Yes	No	-	-	-	12	367	668
4249300289	460	G-05	-	40	No	No	-	-	-	-	-	-
4249330440	425	G-06	-	30	Yes	No	-	-	2	170	875	1,211
4249301419	402	G-07	-	43	Yes	No	-	-	0	354	1,120	1,466
4249301427	425	G-08	-	45	Yes	No	-	-	0	579	1,354	1,751
4249301482	420	G-09	-	75	No	No	-	-	0	-	-	-
4249301064	404	G-10	-	50	Yes	No	-	-	88	781	1,615	2,026
4249331897	406	G-11	-	71	No	No	-	0	338	-	-	-
4249330899	360	G-12	-	40	No	No	-	183	427	-	-	-
4249330730	396	G-13	-	69	Yes	No	-	247	643	1,793	2,669	3,203
4249330757	374	G-14	-	57	No	No	-	377	759	-	-	-

API ID	Datum	Dip Section/ Position	Strike Section/ Position	Number of Sand Picks	GMA 13 BRACS Study	Hargis Study	Depth (Feet) to Top of Aquifers and Formations					
							Yegua Jackson Top	Cook Mountain / Sparta / Weches Top	Queen City Top	Carrizo / Upper Wilcox Top	Middle Wilcox Top	Lower Wilcox Top
4249301889	364	G-15	-	98	Yes	No	-	427	916	2,187	3,152	3,762
4242255301	370	G-16	-	117	Yes	No	-	681	1,251	4,664	5,702	6,467
4242255012	370	G-17	-	93	Yes	No	5	1,347	1,864	4,006	5,129	5,846
4225500110	333	G-18	1-09	81	Yes	No	-	1,879	2,255	3,611	4,612	5,303
4225501235	359	G-19	-	111	No	No	81	2,154	2,700	-	-	-
4225532668	321	G-20	-	103	No	No	450	2,644	3,246	-	-	-
4225500637	246	G-21	-	85	Yes	No	945	3,557	4,340	5,761	6,808	7,665
4225531471	277	G-22	-	0	No	No	1,360	3,868	4,253	-	-	-
4225500270	273	G-23	2-11	96	Yes	No	1,944	4,121	4,714	6,188	7,194	8,042
4225530804	268	G-24	-	51	Yes	No	2,339	4,426	5,087	6,022	7,128	7,963
4225531261	217	G-25	-	33	No	No	2,881	4,906	5,677	-	-	-
4218730412	740	H-01	-	20	No	Yes	-	-	-	-	-	-
4218702989	665	H-02	-	16	No	Yes	-	-	-	-	-	-
4218702991	646	H-03	-	20	No	Yes	-	-	-	-	-	-
4218702992	607	H-04	-	25	No	Yes	-	-	-	-	-	-
4249301921	515	H-05	-	30	Yes	No	-	-	-	85	641	1,014
4249300748	500	H-06	-	3	No	No	-	-	24	-	-	-
4249300917	474	H-07	-	1	Yes	No	-	-	1	302	962	1,318
4249300943	459	H-08	-	1	No	No	-	-	0	-	-	-
4249301920	462	H-09	-	9	Yes	No	-	-	-	568	1,268	1,644
4249300924	501	H-10	-	56	No	No	-	-	-	-	-	-

API ID	Datum	Dip Section/ Position	Strike Section/ Position	Number of Sand Picks	GMA 13 BRACS Study	Hargis Study	Depth (Feet) to Top of Aquifers and Formations					
							Yegua Jackson Top	Cook Mountain / Sparta / Weches Top	Queen City Top	Carrizo / Upper Wilcox Top	Middle Wilcox Top	Lower Wilcox Top
4249300933	466	H-11	-	51	No	No	-	-	12	-	-	-
4249300930	477	H-12	-	63	Yes	No	-	36	119	875	1,573	2,009
4249330236	427	H-13	-	48	Yes	No	-	112	451	1,033	1,800	2,248
4249301068	356	H-14	-	2	Yes	No	-	181	474	1,364	2,123	2,651
4249302003	335	H-15	-	5	No	No	-	412	775	-	-	-
4225500226	350	H-16	-	11	Yes	No	-	580	944	2,197	2,936	3,516
4225500234	377	H-17	-	43	Yes	No	-	705	1,209	2,527	3,318	3,940
4225530774	352	H-18	-	10	Yes	No	-	918	1,449	5,262	6,375	7,187
4225500220	383	H-19	-	16	No	No	-	1,005	1,592	-	-	-
4225531286	387	H-20	-	24	No	No	-	1,233	1,792	-	-	-
4225501373	457	H-21	1-15	46	No	No	280	2,128	2,693	-	-	-
4225530178	482	H-22	-	31	Yes	No	684	2,981	3,484	5,350	6,449	7,350

Table A-3 Depth to top (feet) and thickness (feet) of transgressive shales in the Wilcox Aquifer

API ID	Datum	Rl Shale Top	Rl Shale Thickness	Hb Shale Top	Hb Shale Thickness	Rn Shale Top	Rn Shale Thickness	Kn Shale Top	Kn Shale Thickness	Yk Shale Top	Yk Shale Thickness	Wb Shale Top	Wb Shale Thickness	Td Shale Top	Td Shale Thickness	Du Shale Top	Du Shale Thickness	Psh Shale Top	Psh Shale Thickness
4225500137	329	3,451	147	3,601	15	3,670	13	3,900	13	4,769	24	5,079	22	5,269	77	5,884	6	7,228	78
4225500164	314	3,480	160	3,641	17	3,699	1	3,919	14	4,789	15	5,106	18	5,299	78	5,923	7	7,288	91
4225500178	324	3,446	155	3,600	15	3,665	13	3,861	16	4,756	12	5,050	17	5,254	62	5,869	11	7,213	106
4225500199	377	3,599	100	3,731	8	3,793	18	3,977	18	4,850	10	5,150	21	5,369	40	-	-	7,371	90
4225500243	450	3,760	197	3,993	15	4,054	23	4,210	9	5,050	8	5,363	23	5,588	30	-	-	7,723	144
4225500252	408	3,762	75	3,848	9	3,920	17	4,089	13	4,949	13	5,269	19	5,490	44	-	-	7,560	103
4225500276	301	5,739	407	6,189	34	6,258	43	6,463	6	7,448	12	7,828	12	8,034	42	8,703	33	-	-
4225500279	319	5,747	401	6,192	31	6,256	42	6,466	6	7,456	14	7,836	12	8,046	39	8,708	29	-	-
4225500282	370	5,842	394	6,283	20	6,348	35	6,535	7	7,556	3	7,927	11	8,144	42	8,750	37	-	-
4225500584	419	5,551	390	6,000	27	6,065	24	6,286	11	7,272	17	7,667	15	7,870	56	8,603	32	-	-
4225500586	336	5,502	432	5,985	24	6,046	26	6,266	10	7,304	10	7,675	12	7,889	37	8,550	29	-	-
4225500668	370	3,461	241	3,702	11	3,770	6	4,004	15	4,839	28	5,158	23	5,364	69	5,951	12	7,237	59
4225500707	316	3,530	205	3,736	10	3,777	2	4,042	17	4,912	26	5,219	23	5,427	62	6,024	14	7,190	88
4225500719	299	3,660	198	3,905	5	3,937	15	4,193	18	5,081	12	5,380	24	5,604	55	6,206	21	7,370	68
4225500824	496	3,486	247	3,734	13	-	-	4,075	9	4,973	33	5,276	20	5,508	55	6,107	20	7,161	69
4225500903	409	3,802	104	3,907	7	3,954	13	4,186	18	5,112	12	5,420	18	5,651	53	6,258	17	7,413	83
4225501233	295	3,104	373	3,543	10	3,600	5	3,860	29	4,667	14	4,960	24	5,162	71	5,758	12	7,081	95
4225501295	270	3,623	2,326	5,995	24	6,058	28	6,284	8	7,292	11	7,670	13	7,878	38	8,553	32	-	-
4225530125	491	3,713	1,544	5,264	22	5,333	17	5,580	9	6,643	18	7,005	16	7,229	56	7,909	33	-	-
4225530241	479	2,322	3,529	5,898	27	5,969	18	6,207	12	7,247	14	7,586	10	7,781	57	8,508	40	9,913	41
4225530246	361	4,100	1,883	6,037	19	6,093	27	6,310	11	7,352	4	7,718	14	7,936	36	8,646	35	9,969	45
4225530261	332	5,499	421	5,991	20	6,042	27	6,253	11	7,322	9	7,685	21	7,899	50	8,587	35	9,982	35
4225530587	431	5,502	388	5,940	24	6,002	22	6,219	12	7,265	19	7,658	14	7,859	49	8,568	29	9,845	24
4225531553	405	5,106	1,134	6,294	22	6,352	39	6,555	7	7,568	10	7,966	15	8,152	37	8,761	37	10,198	59

API ID	Datum	Rl Shale Top	Rl Shale Thickness	Hb Shale Top	Hb Shale Thickness	Rn Shale Top	Rn Shale Thickness	Kn Shale Top	Kn Shale Thickness	Yk Shale Top	Yk Shale Thickness	Wb Shale Top	Wb Shale Thickness	Td Shale Top	Td Shale Thickness	Du Shale Top	Du Shale Thickness	Psh Shale Top	Psh Shale Thickness
4225531596	375	5,399	532	6,010	27	6,072	25	6,300	7	7,334	17	7,730	23	7,880	51	8,580	35	9,960	30
4225531660	479	5,829	-1,895	3,936	16	3,999	10	4,266	20	5,189	25	5,513	15	5,740	59	6,353	21	7,433	85
4249300002	473	-	-	-	-	-	-	-	-	-	-	-	-	278	9	-	-	866	32
4249301628	480	-	-	-	-	-	-	-	-	-	-	-	-	411	12	-	-	1,044	36
4249330861	567	-	-	-	-	-	-	-	-	-	-	355	12	465	14	-	-	1,154	35
4249301572	416	-	-	-	-	-	-	-	-	-	-	435	5	539	17	-	-	1,238	37
4249301621	431	-	-	-	-	-	-	-	-	-	-	883	15	965	30	-	-	1,639	61
4249301573	503	11	0	-	-	-	-	-	-	-	-	1,000	17	1,135	23	-	-	1,866	71
4249301310	427	28	152	-	-	-	-	-	-	-	-	1,179	22	1,321	25	-	-	2,143	88
4249301516	412	488	141	-	-	-	-	-	-	-	-	1,537	18	1,679	35	-	-	2,657	77
4249301236	419	576	151	-	-	-	-	-	-	1,499	9	1,730	17	1,871	35	-	-	2,966	63
4249301555	548	722	164	-	-	-	-	-	-	1,729	14	1,989	16	2,128	43	-	-	3,303	56
4249331233	388	1,174	157	-	-	-	-	-	-	2,282	8	2,515	20	2,667	31	-	-	3,940	73
4249301551	371	1,469	223	-	-	-	-	-	-	2,669	15	2,921	17	3,068	41	-	-	4,479	71
4249331621	409	1,896	207	-	-	-	-	-	-	3,217	11	3,484	22	3,642	68	4,212	20	5,181	76
4249330939	423	2,186	243	-	-	-	-	-	-	3,516	24	3,794	26	3,961	73	4,536	30	5,536	72
4249301767	359	2,534	244	-	-	2,851	9	3,092	13	3,944	16	4,238	17	4,408	74	4,999	18	6,075	49
4225500877	421	3,657	246	3,925	12	3,990	8	4,231	14	5,099	26	5,454	17	5,653	75	6,275	23	7,448	80
4225500874	379	3,438	250	3,621	19	3,734	14	3,975	10	4,901	32	5,208	20	5,427	49	6,042	16	7,242	81
4225500858	470	3,850	221	4,069	14	4,132	11	4,392	18	5,340	29	5,659	20	5,890	56	6,510	28	7,631	86
4225530239	451	4,247	161	4,370	14	4,439	13	4,711	12	5,666	23	5,980	18	6,195	64	6,841	31	7,908	79
4225531184	489	2,263	2,555	4,777	23	4,858	10	5,109	11	6,120	19	6,448	22	6,680	50	7,328	35	8,274	66
4225530272	450	5,573	-498	5,176	23	5,251	14	5,491	9	6,522	18	6,825	21	7,075	42	7,760	38	8,707	66
4225531505	472	2,699	2,903	5,637	30	5,710	16	5,958	15	7,017	18	7,374	20	7,628	40	8,348	25	9,601	26
4249330404	470	-	-	-	-	-	-	-	-	-	-	-	-	302	8	-	-	-	-
4249300199	491	-	-	-	-	-	-	-	-	-	-	-	-	376	56	-	-	-	-

API ID	Datum	Rl Shale Top	Rl Shale Thickness	Hb Shale Top	Hb Shale Thickness	Rn Shale Top	Rn Shale Thickness	Kn Shale Top	Kn Shale Thickness	Yk Shale Top	Yk Shale Thickness	Wb Shale Top	Wb Shale Thickness	Td Shale Top	Td Shale Thickness	Du Shale Top	Du Shale Thickness	Psh Shale Top	Psh Shale Thickness
4249300198	468	-	-	-	-	-	-	-	-	-	-	-	-	496	24	-	-	-	-
4249330534	430	-	-	-	-	-	-	-	-	-	-	-	-	617	39	-	-	-	-
4249300289	460	98	52	-	-	-	-	-	-	-	-	-	-	942	49	-	-	-	-
4249330440	425	519	-239	-	-	-	-	-	-	-	-	-	-	1,155	57	-	-	-	-
4249301419	402	249	107	-	-	-	-	-	-	-	-	-	-	1,437	26	-	-	-	-
4249301427	425	240	339	-	-	-	-	-	-	-	-	-	-	1,724	21	-	-	-	-
4249301482	420	522	31	-	-	-	-	-	-	-	-	-	-	1,757	49	-	-	-	-
4249301064	404	647	133	-	-	-	-	-	-	-	-	-	-	1,954	68	-	-	-	-
4249331897	406	858	149	-	-	-	-	-	-	1,861	20	-	-	2,273	55	-	-	-	-
4249330899	360	1,028	233	-	-	-	-	-	-	2,149	25	-	-	2,521	94	-	-	-	-
4249330730	396	1,522	208	-	-	-	-	-	-	2,700	53	-	-	3,104	95	-	-	-	-
4249330757	374	1,655	217	-	-	-	-	-	-	2,913	27	-	-	3,331	73	-	-	-	-
4249301889	364	1,865	241	-	-	-	-	-	-	3,151	18	-	-	3,630	84	-	-	-	-
4242255301	370	4,322	-1,794	2,524	11	2,588	8	2,800	4	3,610	15	3,901	20	4,061	59	4,664	5	5,869	81
4242255012	370	3,710	-227	3,101	12	3,158	-	3,399	11	4,215	25	4,515	22	4,698	73	5,301	7	6,637	86
4225500110	333	3,336	-	3,544	12	3,595	16	3,831	14	4,669	22	4,974	24	5,172	74	5,794	13	7,097	59
4225501235	359	3,292	754	4,021	13	4,088	13	4,298	10	5,156	30	5,498	16	5,689	62	6,320	9	7,631	92
4225532668	321	5,544	-930	4,578	23	4,652	12	4,850	9	5,692	105	6,116	19	6,297	105	6,960	17	8,343	66
4225500637	246	5,418	291	5,680	20	5,734	27	5,950	15	6,799	85	7,318	22	7,510	95	8,235	30	9,593	34
4225531471	277	6,799	-1,228	5,637	22	5,694	26	5,908	8	6,752	36	7,260	17	7,469	66	8,233	18	9,565	25
4225500270	273	5,638	414	6,082	32	6,149	39	6,371	7	7,371	5	7,683	21	7,909	77	8,609	37	10,065	56
4225530804	268	5,476	1,055	6,569	30	6,631	37	6,833	10	7,902	66	8,343	18	8,593	83	9,384	38	11,086	31
4225531261	217	6,135	1,221	7,404	42	7,499	42	7,737	18	9,240	89	9,891	26	-	-	12,094	37	15,435	35
4218730412	740	-	-	-	-	-	-	-	-	-	-	-	-	528	11	-	-	1,169	49
4218702989	665	-	-	-	-	-	-	-	-	-	-	-	-	532	8	-	-	1,253	53
4218702991	646	-	-	-	-	-	-	-	-	-	-	-	-	748	10	-	-	1,531	53

API ID	Datum	Rl Shale Top	Rl Shale Thickness	Hb Shale Top	Hb Shale Thickness	Rn Shale Top	Rn Shale Thickness	Kn Shale Top	Kn Shale Thickness	Yk Shale Top	Yk Shale Thickness	Wb Shale Top	Wb Shale Thickness	Td Shale Top	Td Shale Thickness	Du Shale Top	Du Shale Thickness	Psh Shale Top	Psh Shale Thickness
4218702992	607	-	-	-	-	-	-	-	-	-	-	-	-	828	9	-	-	1,633	52
4249301921	515	-	-	-	-	-	-	-	-	-	-	839	4	963	11	-	-	1,887	47
4249300748	500	19	102	-	-	-	-	-	-	-	-	1,010	11	1,132	11	-	-	2,095	54
4249300917	474	171	132	-	-	-	-	-	-	-	-	1,141	13	1,270	10	-	-	2,229	94
4249300943	459	320	144	-	-	-	-	642	13	-	-	1,344	16	1,471	12	-	-	2,517	92
4249301920	462	415	174	-	-	-	-	759	8	-	-	1,465	17	1,596	10	-	-	2,711	100
4249300924	501	576	113	-	-	-	-	924	15	-	-	1,672	13	1,800	12	-	-	2,958	88
4249300933	466	640	167	-	-	-	-	989	16	-	-	1,753	20	1,884	25	-	-	3,119	81
4249300930	477	672	175	-	-	-	-	1,037	13	1,581	9	1,809	17	1,942	38	-	-	3,216	79
4249330236	427	825	210	-	-	-	-	1,200	18	1,820	21	2,056	14	2,194	31	-	-	3,539	91
4249301068	356	1,095	156	1,257	4	1,312	10	1,475	12	2,202	16	2,413	17	2,559	37	-	-	4,022	90
4249302003	335	1,606	155	1,766	5	1,817	5	1,995	14	2,684	15	2,954	18	3,094	37	-	-	4,683	106
4225500226	350	1,889	152	2,043	7	2,105	8	2,266	10	2,938	14	3,250	14	3,395	38	-	-	5,054	93
4225500234	377	2,169	175	2,350	11	2,426	11	2,603	7	3,318	13	3,651	17	3,818	37	-	-	5,534	102
4225530774	352	4,882	-2,425	2,461	12	2,556	7	2,720	16	3,473	18	3,784	15	3,970	29	-	-	5,811	102
4225500220	383	2,497	181	2,700	11	2,790	9	2,958	16	3,734	15	4,031	20	4,231	27	-	-	6,140	107
4225531286	387	4,518	-1,585	2,928	11	3,020	10	3,181	14	3,990	16	4,297	15	4,490	30	-	-	6,449	104
4225501373	457	5,548	-1,653	3,925	6	4,005	19	4,163	11	4,994	11	5,311	23	5,535	28	-	-	7,632	127
4225530178	482	4,940	-495	4,491	8	4,562	27	4,728	12	5,637	12	5,947	27	6,187	33	-	-	8,259	127